Hydrochemical Characteristics and Groundwater Evolution of a Cambrian Limestone Aquifer, the Northern Territory

By

Jyoti Maggu

Thesis
Submitted to Flinders University
for the degree of

Master of Science
(Groundwater Hydrology)

College of Science and Engineering

30/09/2023

TABLE OF CONTENTS

LIST OF FIGURES

LIST OF TABLES

SUMMARY

The Cambrian Limestone Aquifer (CLA) in the Northern Territory, occupying parts of the Daly and Wiso geological basins is the focus of this study, due to its importance as a water resource, in the semi-arid region of the basins. The Beetaloo sub-basin, located within these basins, has been earmarked for the development of onshore gas due to the vast reserves of gas that it holds. The threats posed from the future development of the gas industry has raised concerns regarding the future of the CLA. This study seeks to provide baseline information on hydrogeological and geochemical processes that influence the water quality of the CLA, which may be used in the future for the management of this valuable resource. The study involves the determination of major regional flow paths and analysis of a large water chemistry dataset (including pH, total dissolved solids and 9 major elements) to better understand the chemical composition of groundwater and to infer the major geochemical processes responsible for variations in water chemistry along regional flow paths. This water quality dataset, compiled from a range of government and industry sources, was used to study the variations in the water chemistry or dominant major ions using a range of commonly employed techniques in hydrochemical studies: correlation matrices, piper diagrams, ionic plots and geochemical modelling. The assessment identifies that regional chemical variations are complex and are a function of several controlling processes, including climatic conditions, recharge locations, groundwater residence times, mixing processes and various water-mineral interactions, with minimal evapotranspiration (ET) effects. Geochemically, the primary control on groundwater chemistry of the CLA is dominated by carbonate reactions owing to its dominant calcite/dolomite mineralogy. Additional processes, such as silicate hydrolysis, cross- formational flows, pyrite oxidation and cation exchange processes are considered important at local scales. This study serves an important basis for understanding the complexity of chemical reactions in the CLA and can be applied to the broader CLA to better inform future management of this valuable resource.

DECLARATION

I certify that this thesis, presented in manuscript form, does not incorporate without acknowledgment any material previously submitted for a degree or diploma in any university; and that to the best of my knowledge and belief it does not contain any material previously published or written by another person except where due reference is made in the text.

Signed.....  .....

Date.....30/09/2023.....

ACKNOWLEDGEMENTS

I would like to express my sincere gratitude to my supervisors, Dr Dylan Irvine and A/Prof Andrew Love for their invaluable guidance in structuring this thesis, their meticulous proofreading of my work and constructive feedback, which have been instrumental in improving the quality of this thesis. I extend a special note of appreciation to Dr Dylan Irvine for his persistent push, drive and motivation, which played a vital role in the successful completion of this thesis. I am greatly thankful to my both supervisors and Flinders University, especially Dr Graziela Miot da Silva, for their unwavering support during challenging periods and for providing me with the extended opportunity to prepare this thesis.

I would also like to acknowledge and extend a special note of thanks to Dr Ritnesh Syna from the Department of Industry, Tourism and Trade. Dr Syna's generous efforts in proofreading this work, providing technical guidance and insightful comments, and engaging in meaningful discussions on the results have significantly enhanced the overall quality and rigor of this thesis.

Furthermore, my sincere gratitude goes to the Northern Territory Department of Environment, Parks and Water Security for generously sharing their raw data, which has served as the basis of this study. I am particularly thankful to Mr. Roderick Johnson and Ms. Lisa Bradly for their understanding and support, and the flexibility they offered, allowing me to take the necessary time off from work to focus on and complete this thesis.

**********HAR HAR MAHADEV**********

1. INTRODUCTION

The Cambrian Limestone Aquifer (CLA), covering over 300,000 km^2 in the Northern Territory, occupies a central position between the Alligator and Finniss regions to the north, Gulf, Elsey and Barkly north regions to the east, Victoria River and Daly regions to the west, and Tanami, Hanson and Sandover-plenty regions to the south (***Figure 1***). Particularly, in arid and semi-arid regions such as the towns of Elliott, Daly Waters, Larrimah, and Newcastle Waters, where surface water is scarce, the CLA serves as the primary water source (Randal, 1973; Evans et al., 2020). Moreover, the CLA maintains perennial flows in the Roper and Flora Rivers throughout the year, concurrently supporting groundwater-dependent ecosystems within Elsey National Park (Tickell, 2005, 2009; Foo and Matthews, 2001; Bruwer and Tickell, 2015).

Figure removed due to copyright restriction

Figure 1 Map of the CLA and Beetaloo Sub-basin extent in the Northern Territory

Grey shaded area represents the extent of the Northern Territory and dark blue represents ocean cover. Data from Department of Environment, Parks and Water Security (DEPWS) (2021a), DEPWS (2023a) and Northern Territory Government (n.d.).

A recent discovery of an extensive unconventional shale gas reservoir within the Beetaloo Sub-basin, located beneath the CLA, raises concerns regarding potential competition between gas enterprises and existing groundwater users. These concerns are detailed in the Scientific Inquiry into Hydraulic Fracturing in the Northern Territory (Pepper et al., 2018). The early-stage exploration of the Beetaloo sub-basin highlights that the water requirements for the development of shale gas extraction is uncertain. Pepper et al. (2018) estimate that Beetaloo gas extraction may require 20,000-60,000 megalitres (ML) of water over 25 years. In this context, the Cambrian Limestone Aquifer emerges as a prospective solution to ensure sustainable water supplies for Beetaloo gas development, although this could adversely impact available water for current users (DEPWS, 2021b). Additionally, the development of Beetaloo gas introduces concerns about contaminating the CLA and other shallower aquifers that overlie the gas targets (Kyalla Formation and Velkerri Formation). Insights from unconventional gas development worldwide, and elsewhere in Australia suggest that aquifer contamination risks may arise from well failures, hydraulic fluid chemicals spills, and excessive saline water resulting from gas development activities (e.g., Leather et al., 2013; Papoulias and Velasco, 2013; Maloney et al., 2017; Patterson et al., 2017). Predicting the likely impacts of Beetaloo gas field development on the CLA requires a detailed understanding of its hydrogeological and hydrochemical characteristics under pre-development conditions as emphasised by the Pepper et al. (2018) scientific inquiry.

The Beetaloo gas field is anticipated to become Australia's largest onshore shale gas field, once fully developed (Scrimgeour, 2016). Its development is projected to contribute over $9 billion to the Australian economy over a 25-year span, while providing cleaner gas to the east Australia market (Deloitte, 2020; TERC, 2020). Recognising the pivotal role this region presents in terms of accelerating economic growth through gas development, extensive investigations have been conducted in recent years. The investigations relevant to this area include the Strategic Regional Environmental and Baseline Assessment (SREBA) program (DEPWS, 2023c), the Geological and Baseline Bioregional Assessment (GBA) program (Department of Agriculture, Water and the Environment, 2021), the Gas Industry Social and Environmental Research Alliance (GISERA) program (CSIRO, 2023) and the Exploring for the Future (EFTF) Program (Southby et al., 2021, 2022; Shamsalsadati, 2022) that have built upon earlier work by Randal (1973), Tickell (2005;

2009), Foo and Matthews (2001), and Tickell and Bruwer (2017). These programs have led to numerous studies in the Beetaloo and wider CLA region to characterise the aquifers overlying the Beetaloo Sub-Basin and improve its hydrogeological conceptualisation (e.g., Fulton and Knapton, 2015; Deslandes et al., 2019; Wilkes et al., 2019; Evans et al., 2020; Orr et al., 2020; Huddlestone-Holmes et al., 2020). Such studies have improved the understanding of recharge processes, as well as the possible mechanisms and pathways that may impact the CLA water quality.

Most studies utilised targeted and small datasets in their investigations, apart from the SREBA program which undertook comprehensive data assimilation from a wide range of published and non-published sources. Despite the wealth of hydrochemical data for the Beetaloo and CLA regions, these studies often employed methods involving assessments of simple ion concentrations and relative abundance plots (e.g., Piper plots) that identified the potential influence of water-mineral interactions on groundwater chemistry. In a broader context, these studies revealed that groundwater in recharge areas typically contains high levels of calcium (Ca^{2+}), magnesium (Mg^{2+}) and bicarbonate (HCO_3^-) ions, whereas areas distant from recharge zones, characterized by longer groundwater residence time, exhibit varying chemical signatures typically dominated by Ca^{2+}, Mg^{2+}, sodium (Na^+), chloride (Cl^-) and sulfate (SO^{2-}) ions (Randal, 1973; DEPWS, 2022a,b). The potential drivers contributing to localised variations in groundwater composition across the CLA have been attributed to the abundance of specific rock minerals, enhanced ET, and potential mixing of water with distinct compositions, drawing evidence from more in-depth studies conducted by Wallace et al. (2018) and de Caritat et al. (2019).

While the connection between groundwater chemistry and the geology that it interacts with is inferred, explicit confirmation and in-depth analysis remains limited for the CLA. The most recent comprehensive analyses of groundwater chemistry and its influencing drivers have been restricted to specific regions including Tennant Creek, Elliott (Wallace et al., 2018) and Lake Woods (de Caritat et al., 2019). These studies revealed that groundwater chemistry aligns with geological patterns and is influenced by ET and mineral weathering processes including the oxidation of sulfide minerals. These findings complement earlier work by Randal (1973) who explored hydrogeochemistry in an extensive area of the northern Wiso Basin and its surroundings. Although Randal (1973) attempted to associate groundwater composition with source rocks and hydraulic conditions, the study lacked a holistic overview of fundamental geochemical processes that

influence groundwater composition.

The limited hydrogeochemical understanding of the CLA present a significant gap in a comprehensive understanding of the drivers and controls affecting water chemistry, and warrants the present study. Given the heightened research interest in the eastern CLA and Beetaloo region, this study targets the less-studied western CLA, stretching westward between Katherine and Tennant Creek (***Figure 2***), and explores the principal groundwater resource in this expanse.

To provide valuable insights into the groundwater origin and its movement through aquifers, hydrogeologists and geoscientists employ several methods and techniques including hydrochemical and environmental isotope techniques (e.g., Clark and Fritz, 1997; Edmunds and Smedley, 2000; De Vries and Simmers, 2002). Isotopic analysis is a well-known tool that enables an understanding of groundwater origins and interactions (Gonfiantini et al., 1998; Gibson et al., 2005), however appropriate isotopic data for the study area is limited (Shand et al., 2022). As such, this study (1) collates a database of the major ion data for the study area and conducts the standard quality control checks, (2) employs widely used major ion data interpretation techniques and fundamental principles of hydrogeology and chemistry to understand the key drivers of groundwater quality evolution. Finally, (3) the groundwater flow patterns of the area are refined and updated to provide essential information about water quality and governing processes along regional flow paths. This study is envisaged to inform the CLA management and aid in safeguarding users against potential impacts from the proposed Beetaloo gas field development.

2. STUDY AREA

The study area encompasses a portion of the Daly and Wiso Basins that geographically spans 15°S to 18°S latitude and 131.5°E to 133.5°E longitude, covering over 65,000 km^2 (***Figure 2***). The area lies to the west of the Stuart highway, near the townships of Katherine, Mataranka, Larrimah, Daly Waters and Elliott. The dominant land uses in the area include beef cattle production and traditional Aboriginal uses (Staben and Edmeadus, 2017). The population density is sparse, numbering fewer than 200 individuals residing within its boundaries, i.e., approximately one person per 325 km^2 (Australian Bureau of Statistics, n.d.).

Figure removed due to copyright restriction

Figure 2 Map of the locations within the study area

Data from DEPWS (2021a) and Northern Territory Government (n.d.).

The terrain is mostly flat to undulating, featuring rounded hills and stony plains (Randal, 1973; ***Figure 3***). The Sturt Plateau, a distinctive geological feature with elevations ranging from 240 to 330 meters above sea level, extends centrally to the east of Top Springs in close alignment with the Buchanan Highway (Foo and Matthew, 2001). Surrounding the study area are geographical peaks: basalt hills to the west (Randal, 1973; Foo and Matthew, 2001), aeolian sand dunes to the south (de Cariat et al., 2019) and bedrock ridge of the Ashburton range to the southeast (Randal, 1973).

Figure removed due to copyright restriction

Figure 3 Map of the Digital Elevation Model (DEM) and major drainage lines of the study area

DEM data from a 1 arc second (~30m) grided digital elevation model (Gallant et al., 2010). Other data from Northern Territory Government (n.d.).

Climatic conditions across the study area display spatial variation from north to south, following the declining trend in annual average rainfall and increase in potential evaporation (Randal, 1973). The Larrimah weather station (15.57 °S, 133.54°E, elevation 180 m AHD), situated

near the northern portion of the study area, typifies a sub-tropical climate with an annual rainfall of 800–1000 mm (primarily during the wet season from December to March), potential evaporation of about 3200 mm and relative humidity ranging from 35% to 65% (BOM, 2020). In contrast, the Elliott weather station (16.25 °S, 133.37 °E, elevation 212 m AHD), located about 225 km to the south of Larrimah, experiences a semi-arid to arid climate characterised by an annual rainfall of 400-600 mm, potential evaporation of approximately 2800 mm and relative humidity of 30 - 50% (BOM, 2020). These climate patterns significantly influence hydrological dynamics and surface water availability across the study area (Randal, 1973; DEPWS, 2022c).

Surface water resources within the study area are scarce, where the Flora River (a tributary of the Daly River) in the northern expanse is a sole permanent surface water body. While perennially flowing waterways are absent from the central and southern areas (south of Daly Waters), certain locations along and near the terminus of waterways (ephemeral in nature) feature near permanent waterholes (Randal, 1973; Fulton and Knapton, 2015). Lake Woods, located in the southern portion of the study area near the township of Elliott, is a large ephemeral lake that can occupy an area of about 1000 km^2 following heavy rains (de Caritat et al., 2019). Verma and Jolly (1992) have highlighted the importance of Lake Woods in terms of providing recharge to the underlying CLA aquifer. The lake is primarily fed by Newcastle Waters Creek to the northeast (***Figure 2***) and runoff from the western flank of the Ashburton Range (***Figure 3***).

2.1 Hydrogeology

The principal groundwater resource in the study area is the CLA, which comprises sequences of sedimentary marine deposits reaching up to 500 m in thickness. These sedimentary strata were deposited during the Cambrian period, about 450-550 million years ago, over a vast expanse through successive sea transgressions and regressions (Verma and Jolly, 1992; Tickell, 2009). The uplifted basement rocks in the region act as natural boundaries to demarcate the extent of the CLA across geological basins (Fulton and Knapton, 2015; Orr et al., 2016). The study area comprises two geological basins: the Daly Basin in the north and the Wiso Basin in the central and southern portions (***Figure 4***).

Hydrogeologically, the CLA is a complex, multilayered groundwater system, with fractured and cavernous rocks (Fulton and Knapton, 2015; Origin, 2016). The CLA can be subdivided into

two primary sub-systems: the upper CLA and the lower CLA. Based on the observed dissimilarity in water levels and quality, Tickell (2018) suggest a lack of vertical hydraulic connectivity between these sub-units within the expanse of the Daly basin, where present.

The upper CLA comprises the aquifer(s) hosted within the Jinduckin Formation, situated along the northeast margin of the study area (***Figure 4***). The Jinduckin Formation mainly consists of siltstone interbedded with numerous thin limestone and sandstone beds (Tickell, 2009). Evaporate minerals such as halite and gypsum/anhydrite occur in this formation (Kruse and Munson, 2013) and contribute to high sulfate proportions and high salinity in groundwater (Tickell, 2011; DEPWS, 2022a). The bore yields are typically less than 5 L/s (Tickell, 2009) and groundwater use in the area is largely limited to stock watering.

Figure removed due to copyright restriction

Figure 4 Map of aquifers extent and crop out areas within the study area. Crop out areas represented by the areas not overlain by Cretaceous sediments

Data from DEPWS (2021a) and Northern Territory Government (n.d.).

The lower CLA comprises aquifers hosted by the Montejinni Limestone of the Wiso Basin and Tindall Limestone of the Daly Basin (***Figure 4 and Figure 5***). Hydrogeologically, the Montejinni Limestone and the Tindall Limestone are the equivalent formations that form an interconnected groundwater system across basin boundaries. These limestone formations comprise predominantly limestone, dolomite and thin interbeds of calcareous siltstone (Randal, 1973). Yields over 20 L/s are common in cavity-dominated areas (Fulton and Knapton, 2015). Groundwater quality within this aquifer is typically of good quality, characterised by a fresh composition (generally TDS ~500mg/L) and with a Ca-Mg-HCO_3 chemical signature (Evans et al., 2020; DEPWS, 2022 a,b).

Figure removed due to copyright restriction

Figure 5 Cross-section Lake Woods to Flora River showing groundwater flow directions (Tickell, 2022)

The Montejinni Limestone or its equivalent in the northern portion, is usually semi-confined, often capped by overlying Cretaceous mudstone and sandstone, as well as recent alluvial and Tertiary deposits (Foo and Matthew, 2001). Outcrops of the CLA are limited to the areas where the Cretaceous sediments are thin or eroded. The CLA outcrops primarily occur along the margins near the Flora River, Dry River, Top Springs and Lake Woods (refer to ***Figure 2***). The dissolution of limestone and weathering of silicate minerals (such as Feldspar) within the Cretaceous sediments have resulted in the formation of sinkholes (Karp, 2002; Evans et al., 2020; Tickell, 2022), which are more common in the northern portion of the study area (Foo and Matthew, 2001).

Recharge mechanisms for the CLA have been explored by Fulton and Knapton (2015) and Evans et al. (2020). Diffuse recharge, macro-pore infiltration, sinkhole recharge, floodout recharge and stream bed infiltration are identified as significant recharge mechanisms. Sinkholes, and open joint and bedding planes in the CLA outcrops, in particular, serve as significant and rapid recharge sources (Randal, 1967; Foo and Matthews, 2001). Due to combined effects of climatic conditions,

surface cover thickness and topography, the northern portion of the study area experiences typically greater and more frequent recharge as compared to the southern portion (Bruwer and Tickell, 2015; Suckow et al., 2018; Deslandes et al., 2019; Crosbie and Rachakonda, 2021). In the central and southern parts of the study area, the recharge areas are limited to the vicinity of Top Springs (Randal, 1973; Foo and Matthew, 2001) and Lake Woods (de Caritat et al., 2019). The variation in recharge rates also influence groundwater quality as particularly evident in the southern portion of the study area. Groundwater from the Montejinni Limestone typically displays brackish to saline characteristics as distance from recharge areas increases (Randal, 1973; Foo and Matthews, 2001; Bruwer and Tickell, 2015).

Groundwater flows mainly from the Montejinni Limestone into the Tindall Limestone that ultimately discharges into the Flora River (Randal, 1973; Tickell, 2011; Amery and Tickell, 2022). Hydrochemical investigation in the vicinity of the Flora River (Irvine and Duvert, 2022) provide evidence to support that a significant portion of the discharge to the Flora River is likely to be sourced from the northern part of the study area (DEPWS, 2022c). In the vicinity of Top Springs area (i.e., central region) where a groundwater mound is present (Tickell, 2022), a minor proportion of groundwater from the Montejinni Limestone discharges to the west into nearby springs, such as Lonely Spring and Palm Spring (DEPWS, 2022b; Tickell, 2022) and to the south into the flow paths of the Camfield River (Randal, 1973; Wilkes et al., 2019; Knapton, 2020). Potentiometric surface maps of the area (Foo and Matthew, 2001; Tickell, 2022) indicate that the horizontal hydraulic gradient is gentle in the southern part of the study area (south of the Buchannan Highway). The hydraulic gradient steepens in the central (Top Springs area) and northern (near Larrimah) parts, corresponding with the narrowing and thinning of the CLA (Foo and Matthew, 2001; Tickell, 2022).

The study area comprises a number of other aquifers hosted by sedimentary deposits and volcanic rocks. A simplified stratigraphic sequence of the aquifers is provided in ***Table 1***. A more comprehensive review of the geology and hydrogeology of these aquifers, along with their interconnectivity is presented in works by Randal (1973), Kennewell and Huleatt (1980), Foo and Matthews (2001), Tickell (2005), Fulton and Knapton (2015), Orr et al. (2020) and Tickell (2022).

Table 1 Generalised hydrostratigraphy of the study area

Data is sourced from Fulton and Knapton (2015) and DEPWS (2022 a,b). Bold and italic text represents the information relevant to the CLA. Terminology describing aquifer scale is broad and based on groundwater travel distance from entry to discharge points (Tickell, 2008): Local scale aquifer = discharge area <5 km; Intermediate scale aquifer = 5 - 50 km; Regional aquifer = >50 km

	Era	Period	Group	Formations	Lithology	Maximum thickness (km)	Yield (L/s)	Hydro-geological relevance	Dominant Water type
Youngest	Mesozoic	Cretaceous	Carpentaria Basin	Undifferentiated	Claystone, siltstone and sandstone	130	0.3 - 4	Local-scale aquifer	***Ca-Mg-HCO_3***
	Paleozoic	***Cambrian***	***Daly***	***Jinduckin Formation***	***Interbedded siltstone, dolostone and sandstone***	***200***	***1 - 12***	***Intermediate- to regional-scale aquifer (CLA)***	***Ca-Mg-SO_4***
				Tindall Limestone or equivalent Montejinni Limestone	***Limestone and dolostone***	***300***	***0.3 - 60***	***Regional-scale aquifer (CLA)***	***Ca-Mg-HCO_3***
			Kalkarindji Igneous Province	Antrim Plateau Volcanics or equivalent Helen Springs Volcanics	Basalt	440	0.3 - 5	Local-scale aquifer / Aquitard	Ca-Mg-HCO_3, Na-HCO_3, Na-Cl-SO_4
			Ungrouped	Unnamed sandstone	Sandstone	150	-	Local- to intermediate-scale aquifer	-
	Neoproterozoic	Tonian/ Cryogenian	Kiana	Cox Formation	Siltstone and shale	450	-	Aquitard	-
				Bukalara Sandstone	Sandstone	75	0.3 - 5	Intermediate- to regional-scale aquifer	NaCl
	Mesoproterozoic	Ectasian	Roper/ Renner	Kyalla Formation	Siltstone and Shale	800	-	Aquitard	-
				Moroak Sandstone	Sandstone	500	0.5 - 5	Local- to intermediate-scale aquifer	NaCl
				Velkerri Formation	Siltstone and Shale	900	-	Aquitard	-
				Bessie creek Sandstone	Sandstone	450	0.5 - 5	Local- to intermediate-scale aquifer	-
Oldest				Corcoran Formation	Siltstone and Shale	>40	<1	Aquitard	-

3. METHODOLOGY

3.1 Data Sources

The data utilised in this study includes major ions (Ca2+, Mg2+, Na+, K+, HCO3-, CO32-, SO42- Cl-), silica (SiO2) and physical parameters including laboratory pH, electrical conductivity (EC) and total dissolved solids (TDS). Laboratory pH was chosen due to the limited availability of field pH records. Where field pH measurements were available, they showed only minor differences, ranging from 0 to 0.3, compared to the laboratory pH measurements.

The groundwater chemistry data used in this study was compiled from a number of sources, including published government databases (DEPWS, 2022d; Schroder et al., 2020), reports (Wilkes et al., 2019; Short, 2021) and non-published sources, such as monitoring data from petroleum industry and Power and Water Corporation. Associated data for sampled bores, including bore construction details, water levels and aquifer extent, were extracted and consolidated from the Department of Environment, Parks and Water Security databases, specifically the following resources: Bore Sites in the Northern Territory (DEPWS, 2021c), SREBA Beetaloo Aquifers (DEPWS, 2023a) and the NT Water Data Web Portal (DEPWS, 2023b).

To aid in the interpretation of groundwater chemistry data, the major ion composition in average seawater data (Appelo and Postma, 1996) and the weighted long-term average rainfall data from nearby sites, Katherine (Galloway et al., 1982) and Tennant Creek (Keywood ,1995), were used. The unpublished surface water chemistry data for the Flora River (G8145021, 14.45 °S, 131.35°E, elevation 91 m AHD) was sourced from the Department of Environment, Parks and Water Security. The surface water sample collected on 16 October 2000 was judiciously chosen to avoid any confounding effects arising from rainfall-induced contributions to the Flora River's baseflow.

3.2 Data quality control

A number of quality control measures were applied to ensure the data collated and used are representative, accurate and complete (**Appendix 1**). In cases where aquifer information for sampled bores was not available, original bore construction reports (DEPWS, 2021d) were inspected to assign aquifers. Additionally, where TDS values were unavailable, the sum of all ions and silica content was applied to ensure dataset coherence.

To ensure that the data are representative of the sampled aquifers, samples from bores installed across multiple aquifers (i.e. bores intercepting CLA and overlying or underlying aquifers), samples with water quality alterations due to sampling methods (i.e. airlifting) or ionic balance error greater than +5% were excluded from the statistical and chemical analyses. As temporal analysis of the data was not considered in this study, for bores with multiple data points, preference was given to the recently collected data.

3.3 Data analysis and interpretation

Water level measurements (up to depths of ~105 m) derived from a network of 20 bores established in the aquifers of Montejinni Limestone and Tindall Limestone were used to infer the groundwater flow paths for the CLA. Due to the seasonally fluctuating nature of groundwater levels, especially in the northern part of the study area over the wet season (DEPWS, 2022c), water level measurements were restricted to the dry season period (from June to early November) and the recent data gathered between 2019 and 2021. To account for the influence of topography on groundwater levels, groundwater elevation was corrected using measured groundwater surface elevations or a high-resolution digital elevation model dataset (1 arc-second Shuttle Radar Topography Mission). The processed groundwater level data was then utilised to create groundwater contours at 5 m intervals using the QGIS software. Following Siegel (2008), contours were drawn by hand to avoid interpretive errors introduced by automated interpolation methods, such as kriging, inverse distance weighting and polynomial regression. The resulting water elevation contours, coupled with the topographic dataset, were subjected to further analysis and interpretation with manually drawn flow paths to deduce the likely location of recharge and discharge areas.

Once the standardized hydrochemical dataset was obtained (see section 3.2), standard approaches commonly used in hydrogeological and hydrochemical studies were employed to inform water quality and governing processes along the flow paths. The data analyses involved computing statistical parameters (maximum, minimum, average, median standard deviation) and Pearson's correlation matrix to discern relationships between variables. To interpret variations in water chemistry in detail (including physical and chemical reactions that occur along the CLA flow paths), a combination of (1) Piper diagrams (Piper, 1944), (2) ionic plots and (3) geochemical

modelling was employed. These three techniques or a combination of them are widely used across hydrogeological and hydrochemical studies (e.g., Love, 2003; Mustapha and Aris, 2012; Sheikhy Narany et al., 2014). The geochemical modelling comprised 23 groundwater samples (two from the Jinduckin Formation, 13 from the Montejinni Limestone and eight from the Tindall Limestone) modelled in PHREEQC Interactive 3.0 (Parkhurst and Appelo, 1999), using phreeqc.dat database. The modelling enabled the calculation of saturation indices (SI) for commonly dissolved species (e.g., calcite, dolomite, gypsum and halite). The SI was calculated in PHREEQC as defined in Equation 1 at 25^{o}C:

$$SI = \log (IAP/K) \quad \text{(Equation 1)}$$

Where IAP is the ionic activity product of the mineral-water interaction and K is the equilibrium solubility constant at a given temperature for particular samples. An equilibrium between mineral and groundwater is indicated when the SI values equal zero. The SI values greater than zero or less than zero indicate that groundwater is oversaturated or undersaturated with respect to a specific mineral, respectively.

To understand the relative contributions of water-mineral interaction and ET processes to the groundwater chemistry at a particular space, a simplified mass balance approach developed by Love (2003) was applied. All major ions (SO_4^{2-},HCO_3^-,Ca^{2+},Mg^{2+},Na^+,K^+) were normalised to a fixed chloride (Cl^-) concentration to account for potential effects of ET, and these were further corrected for rainfall contributions (Equation 2). This analytical method assumes that (1) the sole source of Cl^- in groundwater is rainfall which becomes concentrated by ET in the vadose zone and shallow water table, (2) other major ions vary or concentrate to the same degree as Cl^-, (3) contributions from human influences, continental dust and mixing processes are negligible, and (4) the ion to chloride ratio in seawater is representative of the value in precipitation.

$$Ion_R = Ion_s - [(Cl_r/Cl_s) \times Ion_s] - [Cl_r\,(Ion/Cl)_{sw}] \quad \text{(Equation 2)}$$

Water-mineral interaction | **Sample concentration** | **ET contribution** | **Rainfall contribution**

where Cl_r is the lowest Cl^- concentration of the targeted aquifer, Cl_s is the concentration of Cl^- measured in a given sample, Ion_s is other major ionic concentrations in that sample, $(Ion/Cl)_{sw}$ is the ion to Cl^- ratio in seawater, Ion_R is the concentration attributable to water rock interaction. The samples from the Jinduckin Formation were excluded from this analysis due to limited available records.

4. RESULTS AND DISCUSSION

4.1 Groundwater Flow

Groundwater flow patterns within the study area are influenced by a combination of factors including the topographic and geological features and hydrodynamic conditions. The groundwater elevation contours (***Figure 6***) indicates that the direction of groundwater movement and hydraulic gradients align closely with findings from previous research by Randal (1967), and Foo and Matthew (2001). Generally, groundwater flows from south to north on the western side of the Birdum Creek Fault, which strikes in north-south orientation along the length of the study area boundary (***Figure 6***).

Figure removed due to copyright restriction

Figure 6 Groundwater level contours and inferred flow paths for the Montejinni Limestone and Tindall Limestone aquifers within the study area.

Data from Gallant et al. (2010), DEPWS (2021a) and Northern Territory Government (n.d.).

Notably, groundwater originates from the edges of the CLA near Lake Woods and Top Springs areas in the southern and central-west parts corresponding the northern Wiso Basin. Groundwater from these areas (B-B' and D-D') converge to the northwest of Daly Waters, creating a north-westward flow (E-E') towards the Flora River. This continuous regional flow from south to north (~475 km) reflects the water movement between the overlying Cretaceous sediments and the CLA.

In the central and southern parts (southeast of Daly Waters), where monitoring bores are limited, the groundwater flow patterns are less clear and not well defined (***Figure 6***). This presents uncertainty regarding groundwater flows, particularly for the southern part of the study area. Reports by Fulton and Knapton (2015) and Amery and Tickell (2022) suggest minor flows westward and southward (over less than 10 km) towards the Victoria River Catchment from elevated groundwater zone near Top Springs. These particular westward and southward flows are not presented in ***Figure 6*** as they do not contribute to the regional water flows within the study area and there is no available water quality data along these flow paths.

The interpretation of potentiometric surfaces and terrain also suggests the potential for minor westward flow from the elevated groundwater zone in the Lake Woods area, represented as A-A' in ***Figure 6***. This potential flow path has not been previously documented.

The Sturt Plateau located east of Top Springs, which is a major topographic feature of the study area, appears to significantly contribute to increased recharge along flow-paths C-C' and D-D' by concentrating runoff in low-lying areas. However, no data is currently available to assess its contribution to the CLA's regional flow.

Hydraulic gradients (i.e., slope of the potentiometric surface) can provide a general indication of how quickly groundwater moves, and hence, on residence times. Steeper hydraulic gradients along paths C-C', D-D' and E-E' indicate that groundwater residence times are relatively short in these parts of the CLA compared to the other inferred flow paths. The steeper gradients in these areas correlate with the narrowing and thinning of the CLA (Foo and Matthew, 2001, which is likely to be caused by the uplift of basement rocks (basalt rocks) in adjacent areas (***Figure 4)***. In comparison, the gentle hydraulic gradients along paths A-A' and B-B', corresponding to the widening and thickening of the CLA (***Figure 5***), indicate longer residence times in these areas.

Predicting groundwater residence times in such aquifers is challenging due to the heterogeneity of subsurface (i.e., presence of sinkholes, caves or conduits). Earlier isotopic studies, including the examination of stable isotopes and radioisotopes (Foo and Matthew, 2001; Suckow et al., 2018; Deslandes et al., 2019; Irvine and Duvert, 2022) provide evidence to support that groundwater in the northern part is typically young (recharged less than 2,000 years ago), and has high flow velocities and short residence times compared to the southern part. During the wet season, variations in the potentiometric surface and groundwater residence time may become more noticeable in the northern part (corresponding with the Tindall Limestone region) where recharge is more common.

The interpreted potentiometric surface (***Figure 6***) also provides indication of the areas where recharge and discharge may occur. In line with earlier work by Fulton and Knapton (2015), the potentiometric surface indicates the main areas of recharge are Lake Woods and Top Springs areas, and the primary area where the CLA discharges is the Flora River. Depths to groundwater measured near the Flora River are typically less than 20 metre (DEPWS, 2021d). These identified areas of recharge and discharge, interestingly, align with the outcrop areas of the CLA (***Figure 4***). While measurements of groundwater levels from the Jinduckin Formation (upper CLA) were not included in this study, previous analyses of the water flow measurements from the Flora River by DEPWS (2022a) provide evidence for minor contributions of discharge from the Jinduckin Formation along the 12 km stretch of the Flora River where this formation is near the surface.

4.2 Groundwater chemistry and basic water properties

The distribution of CLA bores included in this study, along with the hydrogeological units that they are screened in, are shown in ***Figure 7***. Groundwater samples from these bores were collected between 1959 and 2021. The bores distribution presented in ***Figure 7*** comprises 9 bores installed in the Jinduckin Formation, 40 bores in the Tindall Limestone and 88 bores in the Montejinni Limestone. Of the total 137 bores, only 53 bores represent high-quality water chemistry data across multiple sampling events. To maintain consistency, the dataset used for interpreting the 137 bores was selected from a single monitoring event **(*Appendix 2*)**, which is representative and closely follows average values for chemical constituents.

Figure removed due to copyright restriction

Figure 7 Map of the water quality monitoring bores locations within the study area

Data from DEPWS (2021a) and Northern Territory Government (n.d.). Bores (77) with poor water quality data are represented as orange points, see more detail in Appendix 1.

Table 2 presents the statistical analyses of the compiled water quality data. Within the CLA, groundwater pH varies from 6.3 to 8.7, indicative of slightly acidic to slightly alkaline conditions. The observed spatial variability in pH values is most likely due to pumping and sampling artefacts impacting on carbon dioxide degassing, and hence, chemical properties (e.g., Appelo and Postma, 1996; Carroll, Hao and Aines, 2009). On average, groundwater pH remains near neutral (~7), aligning with previous studies (e.g., Randal, 1973; Fulton and Knapton, 2015). Compared to rainwater (~4 -5; Keywood, 1995), groundwater pH is higher which is typical for limestone aquifers (e.g., Gabrovšek and Dreybrodt, 2010; Han et al., 2013; Al Kuisi et al., 2015) and indicative of the buffering effect by the dissolved HCO_3^- and CO_3^{2-} species.

Table 2 Statistical summary of hydrochemical data collected from the CLA bores between 1959 and 2021.
EC = electrical conductivity, TDS = Total Dissolved solids, Ca^{2+} = Calcium, Mg^{2+} = Magnesium, Na^{+} = Sodium, K^{+} = Potassium, Cl^{-} = Chloride, SO_4^{2-} = Sulfate, HCO_3^{-} = Carbonate, CO_3^{2-} = Carbonate, SiO_2 = Silica

	pH	*EC (uS/cm)*	*TDS (mg/L)*	*Ca^{2+} (mg/L)*	*Mg^{2+} (mg/L)*	*Na^{+} (mg/L)*	*K^{+} (mg/L)*	*Cl^{-} (mg/L)*	*SO_4^{2-} (mg/L)*	*HCO_3^{-} (mg/L)*	*CO_3^{2-} (mg/L)*	*SiO_2 (mg/L)*
Jinduckin Formation (n=9)			*1970-1999*									
Minimum	7.0	675	390	67	35	9	5	10	11	298	0	12
Maximum	7.6	2410	2230	582	92	18	16	26	1394	616	5	42
Average	7.2	1480	1206	249	68	13	11	16	554	432	0	23
Median	7.2	1010	710	133	72	11	12	12	196	404	0	21
Standard Deviation	0.0	742	820	201	21	4	4	7	602	128	2	9
Tindall Limestone (n=40)			*1969-2021*									
Minimum	6.3	315	215	35	5	2	1	1	0	186	0	18
Maximum	7.8	1492	898	140	52	259	7	339	305	632	1	87
Average	7.1	838	504	104	35	32	3	40	29	498	0	41
Median	7.2	834	505	111	38	14	3	13	17	536	0	39
Standard Deviation	0.4	217	127	29	11	52	1	72	50	108	0	13
Montejinni Limestone (n=88)			*1959-2021*									
Minimum	6.3	474	250	12	24	2	2	2	1.3	317	0	12
Maximum	8.7	6520	4310	258	269	815	80	1436	925	773	23	81
Average	7.4	1222	756	90	49	97	26	116	88	517	0	44
Median	7.4	945	584	85	42	48	22	40	35	511	0	41
Standard Deviation	0.5	861	552	34	30	134	22	201	132	101	3	15

The analysis of groundwater major ion data from the study area shows that the hydrochemistry is heterogeneous. Within the Jinduckin Formation aquifer, anion dominance follows the order: $SO^{2-}>HCO_3^{-}>Cl^{-}$ and cation follow the order: $Ca^{2+}>Mg^{2+}>Na^{+}>K^{+}$ (***Table 2***). The relative high abundance of Ca^{2+} and SO_4^{2-} in the Jinduckin Formation correlates with distinctive minerals confirmed to be present in the aquifer, such as gypsum ($CaSO_4.2H_2O$) and/or anhydrite ($CaSO_4$). Across Tindall and Montejinni limestone aquifers, unsurprisingly, the groundwater anion follows the order: $HCO_3^{-}>Cl^{-}>SO_4^{2-}$. Calcium is the most abundant cation in the Tindall Limestone aquifer. In the Montejinni Limestone aquifer, on average, Ca^{2+} and Na^{+} are almost equally abundant.

Sulfate ion concentrations within the Jinduckin Formation aquifer show large variation between minimum and maximum values (i.e., standard deviation > average), indicating spatial heterogeneity in SO_4^{2-} across the study area. Gamma log available for RN027072 and mapped aquifers extent suggest that bores with low SO^{2-} abundance draw water, at least in part, from the

Tindall Limestone aquifer. The spatial variability in the relative abundance of major ions and its water type classification is shown in ***Figure 8***, along with TDS.

Figure removed due to copyright restriction

Figure 8 Map of TDS and water types spread across the study area

Data from DEPWS (2021a) and Northern Territory Government (n.d.).

The groundwater TDS exhibit notable spatial heterogeneity across the study area, varying from 215 mg/L (Tindall Limestone) to 4,310 mg/L (Montejinni Limestone). As shown in ***Figure 8***, the freshwater zone (TDS < 1000 mg/L) of the groundwater is mainly distributed to the areas characterised by more frequent recharge, such as in the northern region (E-E'), Top Springs (C-C', D-D') and Lake Woods area. Along A-A' and B-B' flow paths, freshwater zone is also represented by the areas receiving localised recharge via runoff from topographic highs (i.e., Sturt Plateau and sand dunes). Groundwater in this zone is classified as the Ca-Mg-HCO3 water types and is represented by 113 bores.

In comparison, slightly to moderately saline water (TDS = 1000 – 10,000 mg/L) is mainly distributed to the south of the Buchanan Highway (Montejinni Limestone aquifer) where TDS appears to be concentrating at discrete locations. As shown in ***Figures 8*** and ***9***, the chemistry of groundwater in this area is typically identified as Na-Cl-SO_4 dominated (7 bores), Ca-Mg-Cl-SO_4 dominated (6 bores), Na-HCO_3 dominated (2 bores) and Na-Cl dominated (1 bore).

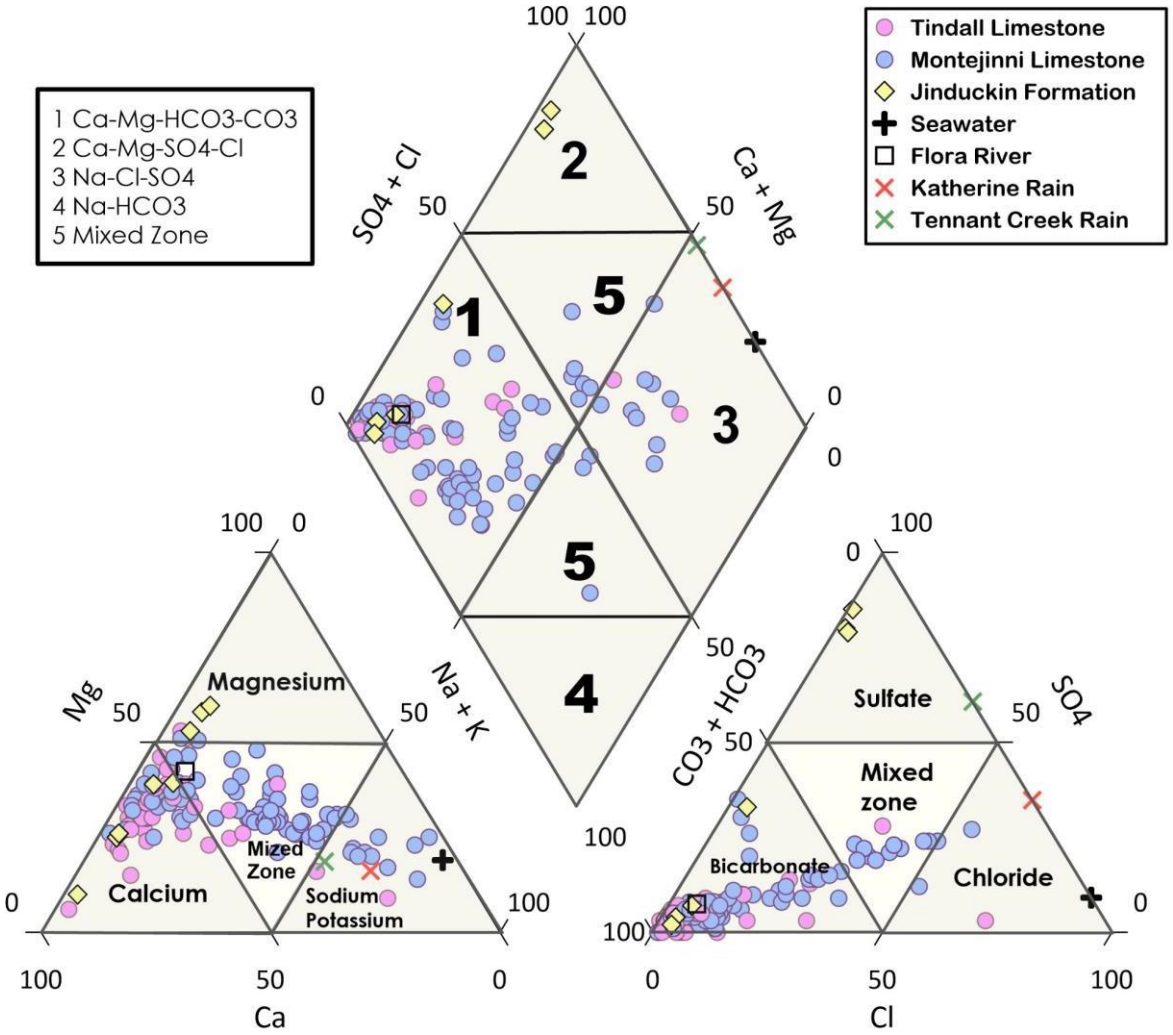

Figure 9 Piper Diagram showing dominant chemical constituents in water samples

Groundwater samples are differentiated by types and aquifers. Mixed water type is represented by Ca-Mg-Cl-SO_4 and Na-HCO_3. Numbers in diamond plot correspond to different water types.

Comparably, the surface water sample from the Flora River corresponds to a Ca-Mg-HCO_3 type, in which Ca^{2+} and Mg^{2+} account for 47% and 42% of the total cation constituents, respectively, and HCO_3^- represents 87% of the total anion constituents. The similarity in chemical compositions between the Flora River sample and nearby Tindall Limestone groundwater, along with the alignment of water table contours (see ***Figure 6***), indicates substantial groundwater

contributions from the Tindall Limestone aquifer. Minor groundwater contributions from the Jinduckin Formation aquifer into the Flora River, as reported by DEPWS (2022a), are supported by the water chemistry results (elevated TDS and Ca-SO_4 type water) from the nearby area shown in ***Figure 8.***

The ionic composition of rainwater, collected from Katherine and Tennant creek regions, is relatively similar despite being collected from widely spaced geographic locations (***Figure 9***). Minor variations in the chemical composition of rainfall are presumed to be linked to solutes originating from continental dust (Appelo and Postma, 1996). Tennant Creek, located further inland compared to Katherine, appears to have a greater contribution from terrestrial sources, as indicated by the relatively higher levels of SO_4^{2-} concentrations observed. To the east of the study area, numerous ephemeral lakes on the Barkly Tableland, including Tarrabool Lake and Lake Sylvester, are underlain and surrounded by bedrock units that contain evaporites (gypsum and halite) (de Cariat et al., 2019). These salt lakes could serve as a significant source contributing to the elevated SO_4^{2-} concentrations observed in precipitation further inland.

Major ion data normalised to chloride is shown in ***Figure 10***, to provide insights into the mechanisms governing the concentration of dissolved ions. Using average seawater data and rainwater compositions as proxies for average regional rainfall, the concentrations of major ions in the surface water and groundwater samples broadly correspond to being derived from processes such as ET and water interactions with minerals (see details in Section 4.3).

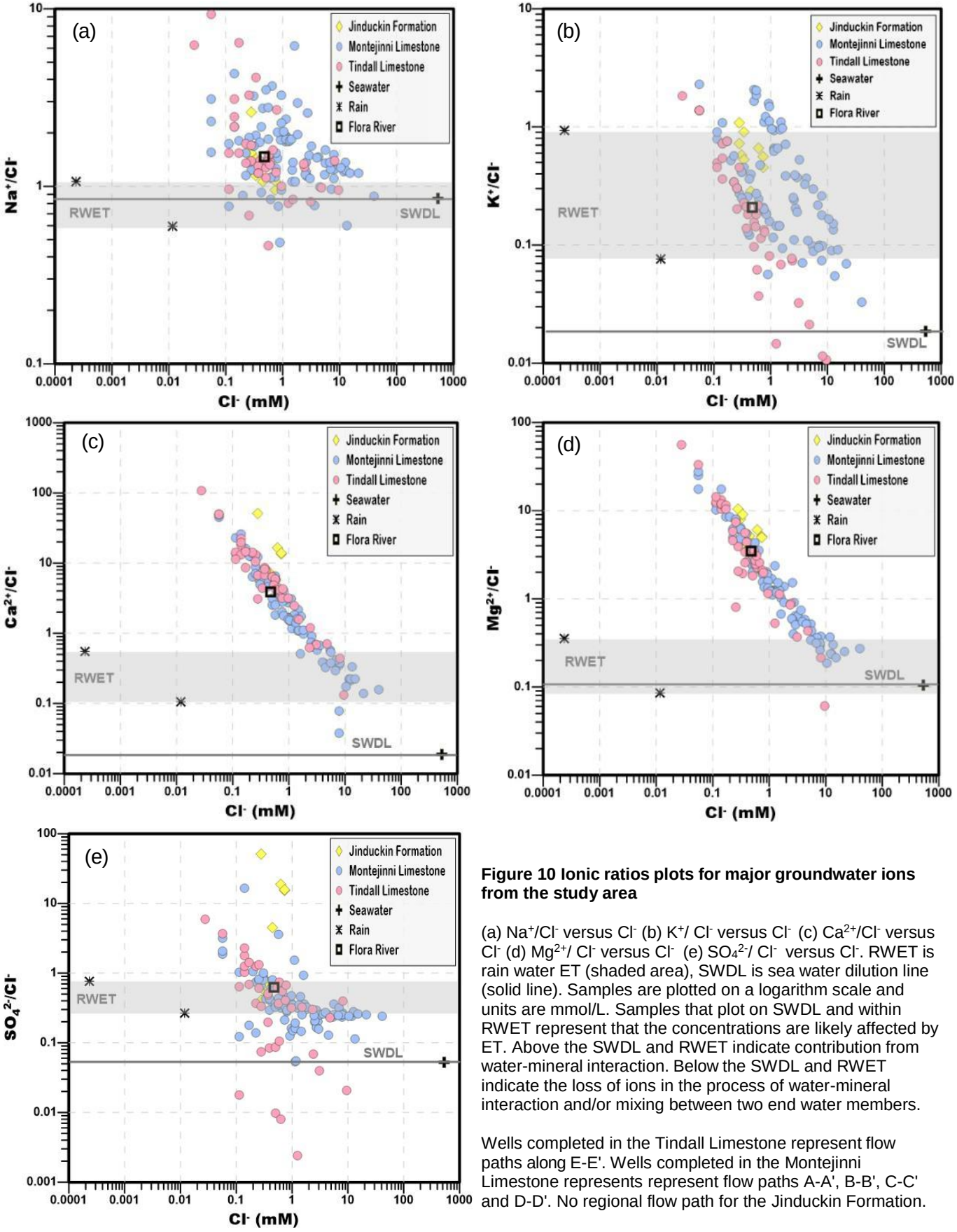

Figure 10 Ionic ratios plots for major groundwater ions from the study area

(a) Na^+/Cl^- versus Cl^- (b) K^+/Cl^- versus Cl^- (c) Ca^{2+}/Cl^- versus Cl^- (d) Mg^{2+}/Cl^- versus Cl^- (e) SO_4^{2-}/Cl^- versus Cl^-. RWET is rain water ET (shaded area), SWDL is sea water dilution line (solid line). Samples are plotted on a logarithm scale and units are mmol/L. Samples that plot on SWDL and within RWET represent that the concentrations are likely affected by ET. Above the SWDL and RWET indicate contribution from water-mineral interaction. Below the SWDL and RWET indicate the loss of ions in the process of water-mineral interaction and/or mixing between two end water members.

Wells completed in the Tindall Limestone represent flow paths along E-E'. Wells completed in the Montejinni Limestone represents represent flow paths A-A', B-B', C-C' and D-D'. No regional flow path for the Jinduckin Formation.

When compared to sea water data (represented by seawater dilution line, SWDL), the normalised concentrations of major ions, are 1 (Na^+) to 5.5 (SiO_2, HCO_3^-) orders of magnitude higher and are indicative of significant enrichment (***Figure 10*** and ***Appendix 3***). Compared to evaporated rainwater (represented as RWET), the measured concentrations of normalised Ca^{2+} (***Figure 10c***) and Mg^{2+} (***Figure 10d***) are notably higher by about 3 to 4 orders of magnitude at lower Cl^- concentrations (<10 mM). This increase in Ca^{2+} and Mg^{2+} concentrations in the Tindall Limestone and the Montejinni Limestone aquifers is indicative of constituents from the dominant aquifer minerals such as calcite and dolomite. Similarly, Na^+ (***Figure 10a***) and SO^{2-} (***Figure 10e***) concentrations are higher by 1 to 3 orders of magnitude at lower Cl^- concentrations.

Consistent with the dominance of gypsum and anhydrite in the Jinduckin Formation (Kruse and Munson, 2013), four bores (RN028162, RN007095, RN008242 and RN007881) screened completely in the Jinduckin Formation show the highest concentrations for Ca^{2+} and SO_4^{2-} relative to Cl^- when compared to the Tindall and Montejinni groundwater samples. Rainwater is typically low in SiO_2 and HCO_3^- concentrations (no data available) and their occurrence in groundwater (***Appendix 3***) at similar concentration levels as other ions (Ca^{2+}, Mg^{2+},Na^+, SO_4^{2-}) confirms the role of water-mineral interactions in groundwater chemistry.

In ***Figure 10e***, most of the SO_4^{2-}/Cl^- molar concentrations remain relatively constant with increasing Cl^- and broadly trend within the RWET that suggests potential effects of regional ET. If the evaporation process is the predominant process impacting chemical constituents, the major ion normalised concentrations are expected to remain unaffected (Jankowaski and Acworth, 1997). However, a downward trend is observed in SO_4^{2-}/Cl^- molar concentrations as Cl^- concentration increases. This downward trend is also noted for Na^+/Cl^-. Further, the reduction in SO_4^{2-} concentration is observed for several groundwater samples from the Tindall Limestone and the Montejinni Limestone at a low Cl^- concentrations (~10 mM). Thus, water- mineral interactions appear to have a significant role in influencing the water chemistry and the ET influence appears to be insignificant.

The overall estimated influence of physical (evaporation) and chemical (water-mineral interactions) processes is presented in ***Figure 11***. By applying equation 1, it can be inferred that water-mineral interactions play a dominant role, contributing to more than 50% of the total chemical

constituents present in groundwater, generally across the study area. There are, however, some exceptions to this pattern, notably in the areas near the Flora River discharge area (to the north), the Antrim Plateau Volcanics along the north-eastern margin and the Buchannan Highway in the central-eastern region. Data analysis for these areas revealed no clear relationship with water depths, topography, and climatic conditions (i.e. rainfall, ET). The estimated potential influence of ET where it likely contributes more than 50% to the water chemistry, appears more closely associated with groundwater dependent ecosystems (GDEs). The GDE atlas (BOM, 2019) confirms a low to moderate potential for GDEs in these areas, with most GDEs concentrated near creeks and drainages lines in the northern region (***Figure 2***). In the area around the Buchanan Highway, where groundwater within the CLA exceeds depths of 50 m from the ground surface, the impact of ET is more likely associated with localised perched aquifers formed within Cretaceous sediments (DEPWS, 2022d) that may be hydraulically connected to the CLA.

Despite the region's semi-arid climate, particularly to the southwest of Daly Waters, which is conducive to evaporation from shallow groundwater (e.g., Lewis et al., 2018), the overall limited influence of ET on groundwater composition is consistent with water depths that typically exceed 20 metres from the surface across the majority of the study area. In areas with shallow groundwater that may favour ET, such as near the Flora River discharge area and Top Springs area, the data does not suggest ET impacts. Given that these areas are groundwater recharge and discharge zones, it is likely that such processes disrupt the ET processes from affecting water chemistry.

Figure removed due to copyright restriction

Figure 11 Estimated effect of ET and water-mineral interaction on groundwater

SWL = Standing water level data from DEPWS (2021c). Other data from DEPWS (2021a) and Northern Territory Government (n.d.). At bore locations where no ET impact is shown, implies the contributions from water-minerals interactions at >50%.

4.3 Possible mechanisms controlling water chemistry

Dissolved major ion species and their compositional relationships in the absence of significant anthropogenic influences can serve as valuable indicators of the sources of solutes and the specific hydrochemical processes contributing to observed water compositions (e.g., Gosseline, 1997; Jalali, 2009; Engle and Rowan, 2013). These compositional correlations among physio-chemical parameters in groundwater are presented in ***Table 3***. Generally, a strong linear correlation (0.7 - 1.0) indicates a significant degree of association between two variables. The linear relationship between variables, however, does not necessarily imply that changes in one variable would cause changes in the other.

In the groundwater samples from the Jinduckin Formation, a strong relationship is evident between TDS and Ca^{2+} (r = 0.98), Na+ (r = 0.98) and SO_4^{2-} (r = 0.99), indicating the substantial contribution to groundwater chemistry from these ions. Similarly, the groundwater samples from the Montejinni Limestone showed a significant positive correlation between TDS and Mg^{2+} (r = 0.90), Na+ (r = 0.96), Cl^- (r = 0.98), SO_4^{2-} (r = 0.97). The strong correlation of Mg^{2+} is consistent with the dolomitic aquifer geology. In contrast, the groundwater samples from the Tindall Limestone displayed weaker correlations between TDS and major ions, implying potential influences from different sources or other processes, such as anthropogenic activities or hydrological dynamics.

Table 3 also reveals notable associations between specific ion pairs. For instance, in the Tindall Limestone aquifer, a notable positive correlation is observed for Ca^{2+} and HCO_3^- (r = 0.81), implying a common origin, such as the dissolution of calcite or dolomite. In the Jinduckin Formation aquifer, a strong positive correlation between Ca^{2+} and SO_4^{2-} (r = 0.99) provides strong evidence to suggest that gypsum dissolution is a major source for both ions. Across all aquifers, Na^+ demonstrates a strong relationship with SO_4^{2-} (r = 0.76 - 0.99), where Na^+ concentration proportionally increase with SO_4^{2-}. This proportional increase in Na^+ and SO_4^{2-} concentrations is indicative of multiple interactions, such as the dissolution of sodium-bearing silicates (e.g., Feldspars), sulfate or sulfide minerals or ion exchange processes with weathered aquifer mineralogy (e.g., with clay minerals).

Table 3 Correlation coefficient matrix of groundwater samples.

Coefficient values more than 0.7 represent strong correlation between ions.

Jinduckin Formation

	pH	*EC*	*TDS*	*Ca^{2+}*	*Mg^{2+}*	*Na+*	*K+*	*Cl^-*	*SO_4^{2-}*	*HCO_3-*	*CO_3^{2-}*	*SiO_2*
pH	1	-0.45	-0.45	-0.47	-0.09	-0.53	-0.03	-0.29	-0.46	0.40	0.13	0.59
EC		1	**1.00**	**0.98**	0.44	**0.98**	0.50	0.64	**0.99**	-0.84	-0.34	-0.50
TDS			1	**0.98**	0.42	**0.97**	0.52	0.64	**1.00**	-0.87	-0.34	-0.51
Ca^{2+}				1	0.25	**0.95**	0.41	0.50	**0.99**	-0.87	-0.32	-0.49
Mg^{2+}					1	0.48	0.57	**0.75**	0.34	-0.12	-0.13	-0.12
Na+						1	0.53	0.69	**0.97**	-0.81	-0.41	-0.59
K+							1	0.66	0.49	-0.54	-0.34	-0.50
Cl^-								1	0.60	-0.62	-0.28	-0.49
SO_4^{-2}									1	-0.89	-0.33	-0.52
HCO_3-										1	0.33	0.61
CO_3^{2-}											1	#N/A
SiO_2												1

Tindall Limestone

	pH	*EC*	*TDS*	*Ca^{2+}*	*Mg^{2+}*	*Na+*	*K+*	*Cl-*	*SO_4^{2-}*	*HCO_3-*	*CO_3^{2-}*	*SiO_2*
pH	1	-0.36	-0.32	-0.35	0.18	-0.32	0.01	-0.35	-0.22	-0.08	0.05	0.12
EC		1	**0.97**	0.43	0.32	0.59	0.23	0.64	0.31	0.42	0.06	0.15
TDS			1	0.51	0.31	0.58	0.21	0.61	0.38	0.46	0.13	0.23
Ca^{2+}				1	0.10	0.00	-0.31	-0.05	0.23	**0.81**	0.20	0.12
Mg^{2+}					1	0.02	0.38	-0.06	0.24	0.57	0.01	-0.13
Na+						1	0.28	**0.97**	**0.76**	-0.21	0.07	0.14
K+							1	0.25	0.22	-0.13	-0.22	-0.12
Cl-								1	0.62	-0.27	0.04	0.10
SO_4^{-2}									1	0.07	0.06	0.02
HCO_3-										1	0.14	0.03
CO_3^{2-}											1	#N/A
SiO_2												1

Montejinni Limestone

	pH	*EC*	*TDS*	*Ca^{2+}*	*Mg^{2+}*	*Na+*	*K+*	*Cl-*	*SO_4^{2-}*	*HCO_3-*	*CO_3^{2-}*	*SiO_2*
pH	1	-0.04	-0.04	-0.49	-0.10	0.07	0.36	0.00	-0.06	-0.22	0.34	0.00
EC		1	**1.00**	0.54	**0.90**	**0.97**	0.50	**0.99**	**0.96**	0.59	0.06	0.30
TDS			1	0.55	**0.90**	**0.96**	0.49	**0.98**	**0.97**	0.58	0.06	0.31
Ca^{2+}				1	0.63	0.37	-0.29	0.52	0.56	0.46	-0.24	0.10
Mg^{2+}					1	**0.81**	0.23	**0.90**	**0.87**	0.62	0.02	0.29
Na+						1	0.60	**0.96**	**0.94**	0.52	0.13	0.27
K+							1	0.47	0.44	0.20	0.24	0.28
Cl-								1	**0.95**	0.46	0.07	0.25
SO_4^{-2}									1	0.49	0.07	0.19
HCO_3-										1	-0.14	0.48
CO_3^{2-}											1	#N/A
SiO_2												1

Despite the marginal impact of ET on groundwater (see section 4.2), interestingly, substantial correlations between Cl^- and one or more ions is observed in the groundwater samples. For instance, strong Cl^- associations is observed with Na^+ in the Tindall Limestone and Montejinni Limestone aquifers; with Mg^{2+} in the Jinduckin Formation and Montejinni Limestone aquifers; and with SO_4^{2-} in the Tindall Limestone and Montejinni Limestone aquifers. These ionic associations also signify complex hydro-geochemical processes such as aquifer recharge or/and evaporative mineralisation that may be present in these aquifers (e.g. gypsum and halite).

Sections 4.3.1 - 4.3.4 below provide insights into the ion association reported above by associating hydrogeochemical processes with aquifers geology and minerals composition.

4.3.1 Carbonate reactions

The higher concentrations of Ca^{2+}, Mg^{2+} and HCO_3^- in most groundwater samples compared to evaporated rainwater or/and seawater dilution line noted above (***Figure 10***) can be reasonably attributed to carbonate dissolution, which is consistent with prior research findings (Wallace et al., 2019). Approximately 76% of the groundwater samples presented HCO_3^-/SiO_2 molar ratios exceeding 10, which provides strong evidence for the significant role of carbonate dissolution in groundwater chemistry (e.g., Hounslow, 1995).

The empirical geochemical relationships between Ca^{2+}, Mg^{2+} and HCO_3^- presented in ***Figure 12a,b***, where groundwater samples plot on and along the 1:2 and 1:4 lines, suggests that the dissolution of calcite ($CaCO_3$) and dolomite ($CaMg(CO_3)_2$) is likely the major sources and influential factors affecting the water chemistry.

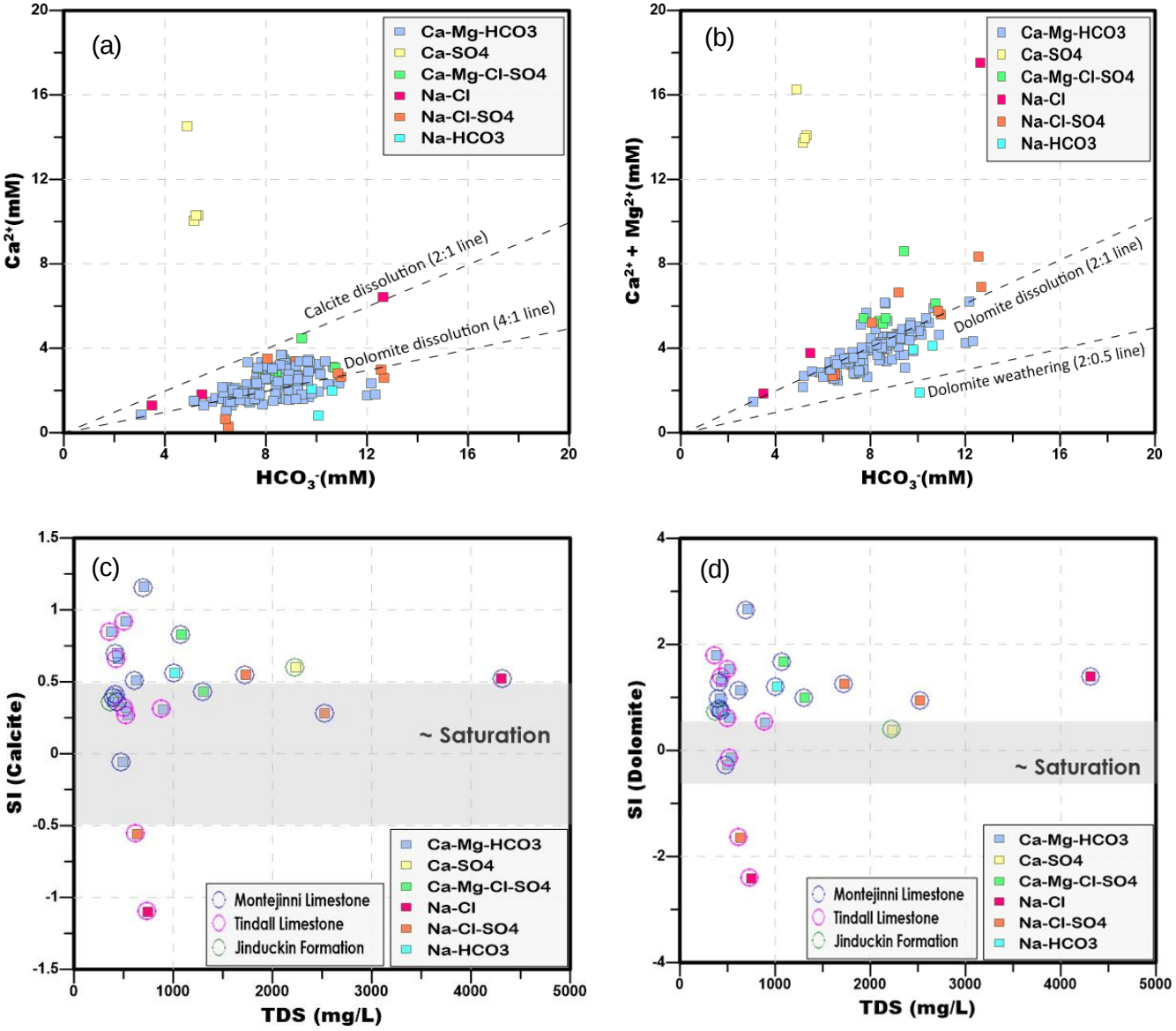

Figure 12 Ionic plots and samples saturation index showing carbonate dissolution

(a) Ca^{2+} versus HCO_3^- displaying calcite dissolution occurring as: $CO_2 + H_2O + CaCO_3 \longrightarrow Ca^{2+} + 2HCO_3^-$ (Appelo and Postma, 1996) (b) Ca^{2+} and Mg^{2+} versus HCO_3^- displaying dolomite dissolution occurring as $CaMg(CO_3)_2 + 2CO_2 + 2H_2O \longleftrightarrow Ca^{2+} + Mg^{2+} + 4HCO_3^-$ and dolomite weathering occurring as $CaMg(CO_3)_2 + CO_2 + H_2O \longrightarrow CaCO_3 + Mg^{2+} + 2HCO_3^{2-}$ (Appelo and Postma, 1996) (c) Calcite saturation index versus total dissolved solids (d) Dolomite saturation index versus total dissolved solids. Shaded area in (c) and (d) represent likely saturation with respect to minerals.

Of carbonates processes noted above, dolomite dissolution is likely the primary contributor, and this is consistent with the known geological presence of dolomite within the local aquifers (Randal, 1973; Kruse and Munson, 2013). Several lines of evidence further support this conclusion:

(1) Ca^{2+}/ Mg^{2+} molar ratios: In approximately 64% of groundwater samples, the Ca^{2+}/ Mg^{2+} molar ratios are close to unity. This alignment is consistent with the characteristics of dolomite dissolution, where the release of Ca^{2+} and Mg^{2+} occurs in approximately equal proportions.

(2) Ca^{2+} /HCO_3- molar ratios: Most groundwater samples show Ca^{2+} /HCO_3- molar ratios approaching 0.25 in ***Figure 12a***, which supports the dolomite dissolution as a

dominant process. This ratio aligns with the stoichiometry of dolomite dissolution reactions.

(3) $(Ca^{2+}+ Mg^{2+})/ HCO_3^-$: A significant proportion of groundwater samples show $(Ca^{2+}+ Mg^{2+})/ HCO_3^-$ molar ratios close to 0.5 in ***Figure 12b***. This further reinforces role of dolomite dissolution, as this ratio reflects the simultaneous release of Ca^{2+} and Mg^{2+} relative to HCO_3^- .

The influence of calcite dissolution, contributing Ca^{2+} and HCO_3^- in the groundwater, is inferred from the Ca^{2+} versus HCO_3^- plot (***Figure 12a***) and Ca^{2+}/ Mg^{2+} molar ratios. In approximately 27% of total groundwater samples Ca^{2+}/ Mg^{2+} molar ratios are close to 2, indicating a potential influence of calcite dissolution (e.g., Mayo and Loucks, 1995; Barzegar et al., 2018), especially in the Tindall Limestone aquifer (represented by 50% of the samples). The reported sporadic distributions of dolomite minerals within the Tindall Limestone Formation (e.g., Randal, 1973) support that calcite dissolution may play a more significant role in this aquifer.

The PHREEQC modelled SI using concentrations of groundwater samples confirm that dolomite and calcite dissolution are the primary factors influencing the water chemistry in the study area. The modelled concentrations indicate that the groundwater is typically in equilibrium (SI = -0.5 to 0.5) or oversaturated (>0.5) with respect to both dolomite and calcite (***Figures 12c and 11d***). The observed near saturation for Ca-Mg-HCO_3 suggests that even in low TDS areas (corresponding to recharge areas), calcite and dolomite may rapidly precipitate given that groundwater in the area is relatively undisturbed and in equilibrium to near-equilibrium conditions. Geochemically, this process would be dominant when the pH of the groundwater system is buffered by the CO_3^{2-} and HCO_3^- species and the observed pH range of 6.3 - 8.7 falls within the HCO_3^- and CO_2 equilibrium zone (Appelo and Postma, 1996).

Exceptionally, two water samples from the northern part of the study area (corresponding to the Tindall Limestone aquifer), characterised as Na-Cl and Na-Cl-SO_4, were found to be undersaturated with respect to dolomite and calcite. The undersaturation of these minerals suggest that additional processes other than the dissolution of calcite or dolomite contribute to the presence of Na^+, Cl^- and SO_4^{2-} in this specific region. The likely source for these ions is potentially the underlying basalt formation, known as the Antrim Plateau Volcanics, which has been documented to contain high Na^+ (15,000 to 27,000 mg/L) and SO_4^{2-} concentrations (up to 2,000 mg/L) (Randal,

1973; Fulton and Knapton, 2015). A recent hydrochemical investigation by Irvine and Duvert (2022) also provide evidence that some nearby boreholes draw water from the Antrim Plateau Volcanics, either partially or wholly, as the screen depths of these boreholes are situated below the base of the Tindall Limestone Formation. The low TDS value in locations are believed to result from dilution, likely due to significant recharge events and rapid throughflow processes.

The inverse correlation observed between HCO_3^- and other ions in samples from the Jinduckin Formation (***Table 3***) suggests that HCO_3^- is being net removed from the aquifer. This may be due to the oversaturation of calcite in the aquifer (***Figure 12c***), which could have led to increased mineral precipitation and the subsequent removal of HCO_3^-.

Figures 12a and ***12b*** reveal an excess of HCO_3^- relative to Ca^{2+} and Mg^{2+}, which is likely originating from sources other than the concurrent dissolution of calcite and dolomite. This excess HCO_3^- is postulated to result from feldspar dissolution, as discussed in section 4.3.2.

4.3.2 Silicate weathering / Sodium sources

The observed increase in Na^+(***Figure 10***) , as well as elevated HCO_3^- and SiO_2 levels (**Appendix 3)** can be attributed to the incongruent dissolution of silicate minerals such as feldspar or K-bearing minerals (e.g., muscovite, phengite), which is consistent with several thin interbeds of siltstone and sandstone lithologies in the local aquifers (DEPWS, 2022 a,b). This process is commonly described as the hydrolysis of aluminosilicate (e.g., Hounslow, 1995):

$$\underset{\text{(Albite)}}{2NaAlSi_3O_8} + \underset{\text{(Carbonic acid)}}{2H_2CO_3} + 9H_2O \longrightarrow \underset{\text{(Kaolinite)}}{Al_2Si_2O_5(OH)_4} + 2Na^+ + \underset{\text{(Silicic acid)}}{4H_4SiO_4} + 2HCO_3^-$$

For Ca-Mg-HCO_3 classified waters, the surplus of Na^+ relative to Cl^- at lower Cl^- concentrations (<10 mM) in the plot of Na^+ versus Cl^- (***Figure 13a***) suggests that Na^+ originates from processes unrelated to halite dissolution (Hounslow, 1995) which is consistent with the geology of the Tindall Limestone and the Montejinni Limestone aquifers. Sodium ion for these waters likely comes from the weathering of Na- and K- rich minerals or through secondary processes, such as cation exchange (e.g., Edmunds et al., 2003; Appelo and Postma, 1996; see section 4.3.3). The influence of silicate weathering on groundwater chemistry is evident from the plots of (Na^+ and K^+) versus total cations and (Ca^{2+}+Mg^{2+}) versus total cations presented as ***Figure 13c*** and ***Figure 13d***, respectively. These plots provide empirical evidence of silicate weathering, as indicated by some Ca-Mg-HCO_3 classified data points (15%) that follow the 2:1 line in both plots.

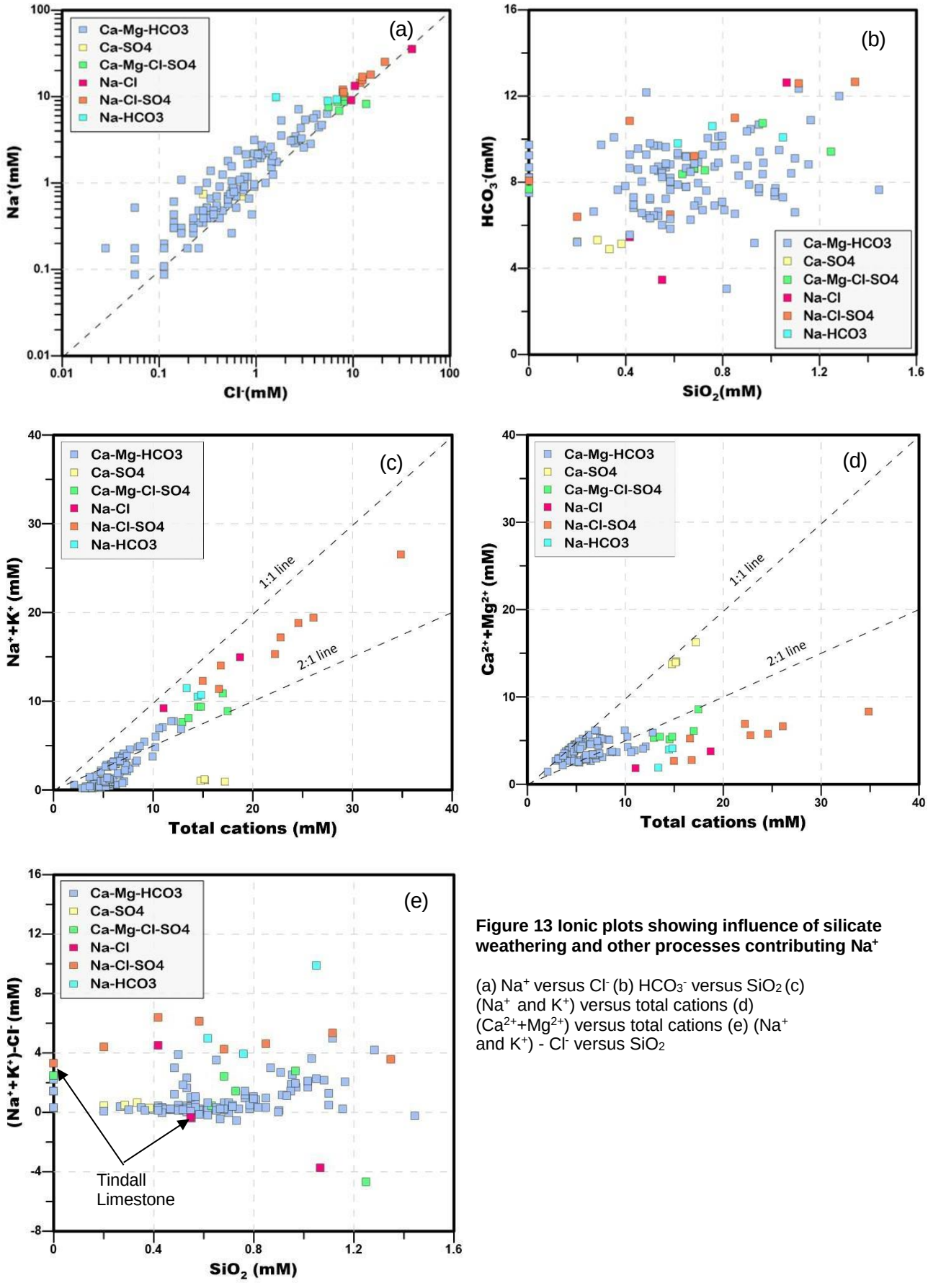

Figure 13 Ionic plots showing influence of silicate weathering and other processes contributing Na^+

(a) Na^+ versus Cl^- (b) HCO_3^- versus SiO_2 (c) (Na^+ and K^+) versus total cations (d) (Ca^{2+}+Mg^{2+}) versus total cations (e) (Na^+ and K^+) - Cl^- versus SiO_2

Groundwater samples characterised as Ca-Mg-Cl-SO_4, Na-Cl-SO_4, Na-Cl and Na-HCO_3 related to flow paths A-A' and B-B' (see ***Figure 6***), align along the 1:1 line in the Na^+ versus Cl^- plot (***Figure 13a***), indicating a close correlation between Na^+ and Cl^-. In the Montejinni Limestone aquifer (flow paths A- A' and B-B'), three geochemical processes may explain this relationship and the source of Na^+:

(1) direct silicate weathering that releases Na^+ into the water as a result of the known interbedded sandstone and siltstone lithologies in the local aquifers (DEPWS, 2022a,b). Supporting evidence for this process is shown in ***Figure 13e*** where (Na^+ and K^+) is in excess compared to Cl^- for these particular water types.

(2) indirect processes involving the removal of Ca^{2+} and Mg^{2+} in ion exchange processes (see section 4.3.3) or through the precipitation of calcite or dolomite (see section 4.3.1) that results in consequential enrichment in Na^+ concentrations compared to Ca^{2+} and Mg^{2+}. Evidence for this process is visible for these water types in ***Figures 13c*** and ***13d***.

(3) cross-formation sources located in the vicinity of A-A' and B-B' flow paths. The observed strong correlation between Na^+ and other ions such as Cl^-, Mg^{2+} and SO_4^{2-} in the Montejinni Limestone aquifer (***Table 3***) suggests three potential cross-formational sources, including:

- **Hooker Creek Beds Formation**: Hooker Creek Beds Formation is stratigraphic equivalent of the Jinduckin Formation (upper CLA) in the central and southern parts of the study area (underlain by the Wiso Basin) and known to contain gypsum and halite as main minerals (Kruse and Munson, 2013). While earlier reports (Foo and Matthew, 2001; Tickell, 2022) have indicated erosion of Hooker Creek Beds in this area, there is a possibility that remnants of this formation may still exist within the unsaturated zone and are influencing the water quality of the Montejinni Limestone aquifer during the precipitation infiltration.
- **Anthony Lagoon Formation**: Anthony Lagoon Formation is stratigraphic equivalent of the Jinduckin Formation (upper CLA) and located in the adjacent eastern basin (Georgina Basin). This Formation is also known to contain gypsum and halite as primary minerals (Kruse and Munson, 2013). Given there are

observed similarities in water chemical compositions (DEPWS, 2022b) and water levels (Amery and Tickell, 2022) in the adjoining Georgina Basin, there are possibilities for lateral exchange between basins through preferential flow paths in the Birdum Creek fault zones (***Figure 6***).

- **Basement rocks (Renner group):** Basement rocks contain saline fluid (Randal 1973; Fulton and Knapton, 2015) and are considered a potential source, since basalt aquitards are thin or absent in this area (Fulton and Knapton, 2015) that suggest the possibility of upward solute migration due to density-driven gradient flows.

The under-saturation of halite associated with Ca-Mg-Cl-SO_4, Na-Cl-SO_4, Na-Cl and Na-HCO_3 classified water provides further evidence that there are no major sources of halite in the Montejinni Limestone. However, further detailed investigations are required in this area to confirm the specific processes that are at play along the flow paths A-A' and B-B'.

Apart from releasing cations (Na^+, K^+, Ca^{2+}, Mg^{2+}) and HCO_3^-, silicate weathering introduces silicic acid (H_4SiO_4), a precursor for the formation of SiO_2. Measured SiO_2 concentrations in the Jinduckin Formation aquifer, the Tindall Limestone aquifer and the Montejinni Limestone aquifer average 23 mg/L, 40 mg/L and 43.82 mg/L, respectively (***Table 2***). The modelled SI indicated that almost all groundwater samples are saturated or oversaturated with respect to quartz (0.08<SI>0.72) and chalecedony (-0.04<SI>0.29) while being under saturated with respect to amorphous SiO_2 (-2.8<SI>-0.55). Despite the relatively high solubility of amorphous silica (non-crystalline form of SiO_2), this difference in mineral saturation implies that quartz and chalecedony dominates the local aquifers, and are the main sources contributing additional dissolved SiO_2 to groundwater. This observation is consistent with the aquifers geology (Randal, 1973; Smith, 2016).

Bicarbonate ion and SiO_2 do not display a clear relationship in ***Figure 13b***, which is indicative of multiple competing geochemical processes that are at play within local aquifers and affect the concentrations of HCO_3^- and SiO_2 in groundwater. The excess of HCO_3^- compared to SiO_2 can be attributed to three key factors: (1) the relative abundance of carbonate minerals compared to silicate minerals in local aquifers; (2) the higher solubility of carbonate minerals compared to silicate minerals, contributing to increased HCO_3^- in groundwater, and (3) multiple geochemical processes

such as carbonates dissolution and silicate weathering, occurring in local aquifers that simultaneously release HCO_3^- in groundwater.

Examination of ***Figure 12b*** suggests that where HCO_3^- is deficit compared to Ca^{2+}, Mg^{2+} (or Na^+), this is likely to be balanced by Cl^- and SO_4^{2-}. This pattern is particularly noticeable for the Ca-Mg-Cl-SO_4 and Na-Cl-SO_4 water types along flow paths A-A' and B-B' that generally fall above the 1:2 line.

4.3.3 Ion exchange

The ion exchange effects across the study area were examined using bivariate plots of (Ca^{2+}+Mg^{2+}-HCO_3^--SO_4^{2-}) versus (Na^+-Cl^-) (***Figure 14a***) and (Ca^{2+}+Mg^{2+}) versus (HCO_3^-+SO_4^{2-}) (***Figure 14b***). The linear slope of -1.1 for groundwater samples on the plot of (Ca^{2+}+Mg^{2+}-HCO_3^--SO_4^{2-}) versus (Na^+-Cl^-) indicates that Ca^{2+}, Mg^{2+} and Na^+ concentrations are interrelated through ion exchange. The strong correlation between these ions, particularly for samples from the Jinduckin Formation and Montejinni Limetsone aquifers (***Table 3***), supports this postulation.

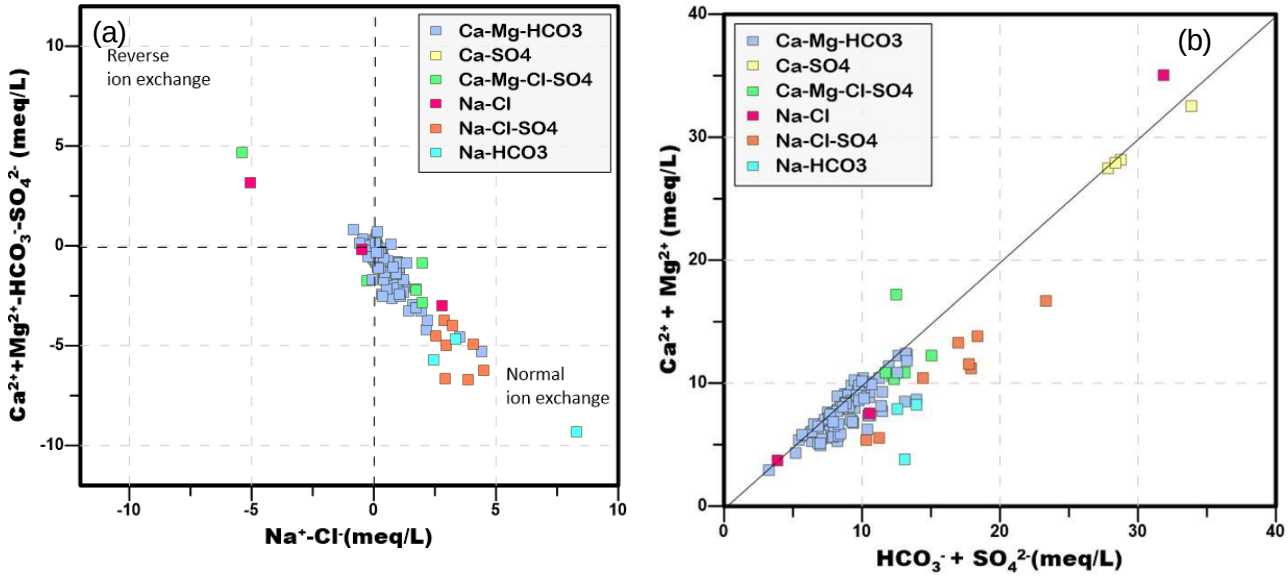

Figure 14 Ionic plots showing the cation exchange process

(a) (Ca^{2+}+Mg^{2+}-HCO_3^--SO_4^{2-}) versus (Na^+-Cl^-) displaying concentrations of (Ca^{2+}+Mg^{2+}) and Na^+ involved in exchange reactions with (HCO_3^--SO_4^{2-}) and Cl^-, respectively. (b) (Ca^{2+}+Mg^{2+}) versus (HCO_3^-+SO_4^{2-}). Normal ion exchange process occurs as: $2Na^+$-Clay(s) + Ca^{2+} (aqueous) $\longrightarrow$ Ca^{2+}-Clay(s) + $2Na^+$ (Hounslow, 1995). Reverse ion exchange process occurs as Ca^{2+}-Clay(s) + $2Na^+$ (aqueous) $\longrightarrow$ Na_2-Clay(s) + Ca^{2+} (Hounslow, 1995)

Groundwater predominantly undergoes normal ion exchange, releasing Na^+. This observation corresponds with the presence of clay minerals, such as kaolinite, that has been reported in equivalent limestone lithologies in the adjacent Georgina Basin (Smith, 2016). These clay minerals generally form as a result of incongruent dissolution of silicate minerals and can

significantly influence water chemistry through surface interactions and ion exchange mechanisms (e.g., Kowalska, Güler and Cocke, 1994). The influence of ion exchange is likely more pronounced in areas where surface water infiltrates through clay sediments, such as around Lake Woods area (de Cariat et al., 2019), or where groundwater residence times are longer which enable for longer interactions between groundwater and rock minerals. This interaction is evident along the flow paths A-A' and B-B', where groundwater transitions from Ca-HCO_3 or Ca-Mg-HCO_3 types into Na- HCO_3, Na-Cl-SO_4 and Na-Cl types (***Figure 8***).

Further, ***Figure 14b*** shows a deficiency of (Ca^{2+}+Mg^{2+}) compared to (HCO_3^-+SO_4^{2-}) for water samples characterised as Na-Cl-SO_4, Ca-Mg-Cl-SO_4, Na-HCO_3 types. This deficiency is likely compensated by Na^+, released during processes such as silicate weathering, mixing processes or ion exchange mechanisms. Some degree of reverse ion exchange may also occur locally, as indicated by the excess Ca^{2+} and Mg^{2+} concentrations in samples classified as Ca-Mg-Cl-SO_4 and Na-Cl types, which plot above the 1:1 line in the (Ca^{2+}+Mg^{2+}) over (HCO_3^-+ SO_4^{2-}) plot.

4.3.4 Gypsum dissolution

For $CaSO_4$ classified water within the Jinduckin Formation aquifer, the elevated concentrations of Ca^{2+} and SO_4^{2-} (***Figure 10***), along with a strong correlation observed between these ions (***Table 3***), are consistent with the dissolution of evaporative sulfosalt minerals, such as gypsum ($CaSO_4.2H_2O$) and/or anhydrite ($CaSO_4$) (***Figure 15a***). Given the relatively high solubility of gypsum (Appelo and Postma, 1996), these water types are associated with high TDS levels (1,970- 2,230 mg/L). The saturation index for gypsum presented in ***Figure 15b*** confirm that gypsum dissolution is the primary factor influencing the water chemistry within the Jinduckin Formation. The bores that draw water from the Tindall and Montejinni Limestone aquifers partly or wholly consistently show undersaturation for gypsum at all salinities.

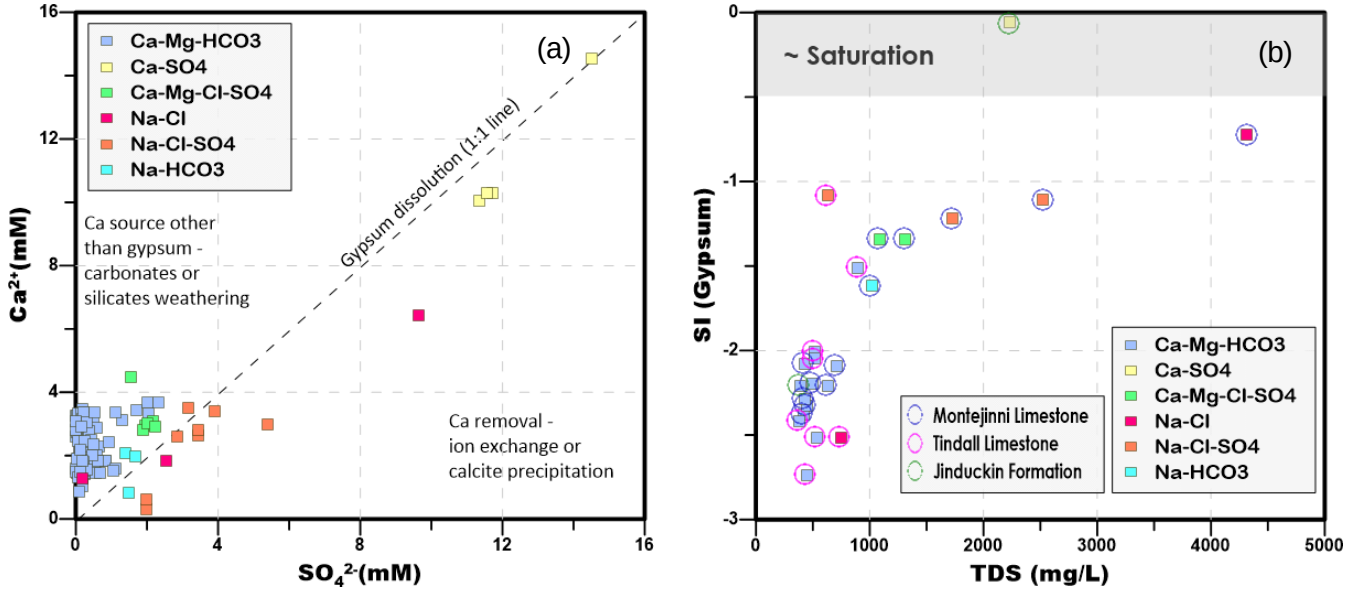

Figure 15 Ionic plot and samples saturation index showing gypsum dissolution

(a) Ca^{2+} versus SO_4^{2-} displaying gypsum dissolution occurring as $CaSO_4.2H_2O \longrightarrow Ca^{2+} + 2H_2O + SO_4^{2-}$ (Appelo and Postma, 1996) (b) Gypsum saturation index versus total dissolved solids

In the Montejinni Limestone aquifers, the dominance of SO_4^{2-} is represented by Na-Cl-SO_4 and Ca-Mg-Cl-SO_4 water types (***Figure 8***). The possible source of SO_4^{2-} in these water types could be associated with the evaporite sulfosalt minerals (e.g., gypsum and/or anhydrite) contribution from the Hooker Creek Beds and the Anthony Lagoon Formation. These formations may contribute solute to the Montejinni Limestone aquifer through processes including mixing, diffusion and aquifer recharge (see section 4.3.2 for detail). An additional potential source of SO_4^{2-} could be sulfer bearing minerals, such as pyrite, which have been reported in lithologies equivalent to the CLA in the neighbouring eastern region (e.g., Kruse & Radke, 2008). Furthermore, the infiltration of precipitation containing sulfate salts originating from salt lakes (Keywood, 1995) may also introduce SO_4^{2-} to the groundwater, though this process is not considered significant.

Figure 15a presents relatively lower or marginal concentrations of SO_4^{2-} compared to Ca^{2+}, particularly in Ca-Mg-HCO_3 water types. This lower SO_4^{2-} concentration could result from one or more factors, including (1) the reduction of SO_4^{2-} to sulfide ions (S^{2-}), likely facilitated by specific types of bacteria under anaerobic conditions, or/and (2) the excess of Ca^{2+} contributed by processes like carbonates dissolution, silicate weathering or cation exchange, as discussed earlier.

In comparison, groundwater samples from the Jinduckin Formation classified as $CaSO_4$ (3) and those from the Montejinni Limestone aquifer, particularly classified as Na-Cl-SO_4 (7), show slight Ca^{2+} depletion relative to SO_4^{2-} (***Figure 15a***). This Ca^{2+} depletion corresponds to the

precipitation of carbonates (see section 4.3.1, ***Figure 12d***), where Ca^{2+} is removed from the groundwater.

5. GEOCHEMICAL MODEL OF THE CLA

5.1 Presentation of the conceptual model

During the wet season (November - April), moisture-laden air, carrying a diluted seawater signature, moves inland and combines with terrestrial dust and aerosol particles that influence the chemical composition of inland rainwater (***Figure 9***), and hence recharge water quality (Wilkins et al., 2022). Rainwater compositions closest to the coast resemble diluted seawater signature (Na-Cl), whereas those further inland, represented by Katherine and Tennant Creek rainwater compositions, show an enrichment in ions besides Na^+ and Cl^- (***Figure 10***).

To better understand the changes in water quality across the study area, groundwater quality was assessed along regional flows paths influenced by climatic conditions, topography and geological structures. The observed variance in water quality along these flow paths, where major ions to chloride ratios deviate significantly (3 - 5.5 orders of magnitude) from seawater and rainwater data, provide compelling evidence for various water-mineral interactions as the primary drivers of water quality. Importantly, the influence of ET on major ion chemistry remains limited, primarily due to groundwater depths generally exceeding 20 meters from the surface across the study area (***Figure 11***).

Within recharge zones, represented by the southeastern, central-western regions (parts of the Montejinni Limestone aquifer) and the northern region (all Tindall Limestone aquifer), mildly acidic rainwater (pH ~5) evolves to a neutral or slightly alkaline pH (6.3 - 8.7) which suggests an interaction between recharged water and aquifer minerals. Carbonates are the major aquifer material within the CLA, and an assessment of water chemistry data (statistical analyses and Piper diagram) indicates that the CLA is dominated by a Ca/Mg-HCO_3 signature, and pH in this region is primarily buffered by the HCO_3^- and CO_3^{2-} species. PHREEQC modelling, aimed at determining specific mineralogical controls on water chemistry, confirms that dolomite and calcite play pivotal roles in influencing water chemistry even at low TDS values (***Figures 12c*** and ***12d***), which is consistent with its residence times (water age of 260 - 7,800 years before present; Foo and Matthew, 2001) and the higher solubility of carbonate minerals.

However, in the northern region near the basaltic high zone (E-E' flow path), saturation

indices for dolomite and calcite are below zero for groundwater quality characterized as Na-Cl and Na-Cl-SO_4, which suggests that these minerals are not the primary drivers of the observed water quality. Instead, this distinct chemical composition in the northern region reflects a localized influence (i.e., diffusion of solutes) from the underlying Antrim Plateau Volcanics. In other parts of the CLA, elevated levels of dissolved potassium and sodium in bores are attributed to a combination of one or more processes, including silicate weathering processes, cation exchange processes, carbonates precipitation, and mixing processes.

Areas with poor recharge conditions, represented by discrete locations within the central-east and southwest regions (parts of the Montejinni Limestone aquifer), show various water types, including Na-HCO_3, Ca-Mg-Cl-SO_4, Na-Cl-SO_4 and Na-Cl. In these areas, the excess of Ca^{2+}, Mg^{2+} and Na^{+} combined with elevated Cl^{-} and SO_4^{2-} levels in groundwater appear to evolve from low salinity Ca-Mg-HCO_3 type waters as a result of several geochemical processes other than dolomite and calcite dissolution and precipitation, including pyrite oxidation, silicate weathering (specifically Feldspar), ion exchange, mixing of different composition waters (***Figure 16***), or/and the deposition of salt-lake derived aerosols. Ion exchange process is considered significant at local scale.

Surface water compositions of the Flora River closely resemble those of nearby Tindall Limestone groundwater, indicating substantial groundwater contributions to the river.

Geological studies for the Jinduckin Formation (Kruse and Munson, 2013) indicate the presence of evaporative sulfosalt minerals (i.e., gypsum and/or anhydrite) which play an important role in influencing the water chemistry (Ca-SO_4) at a local scale. The distinctive water chemistry of the Jinduckin Formation confirms its relatively lower contribution to the river's overall chemical composition.

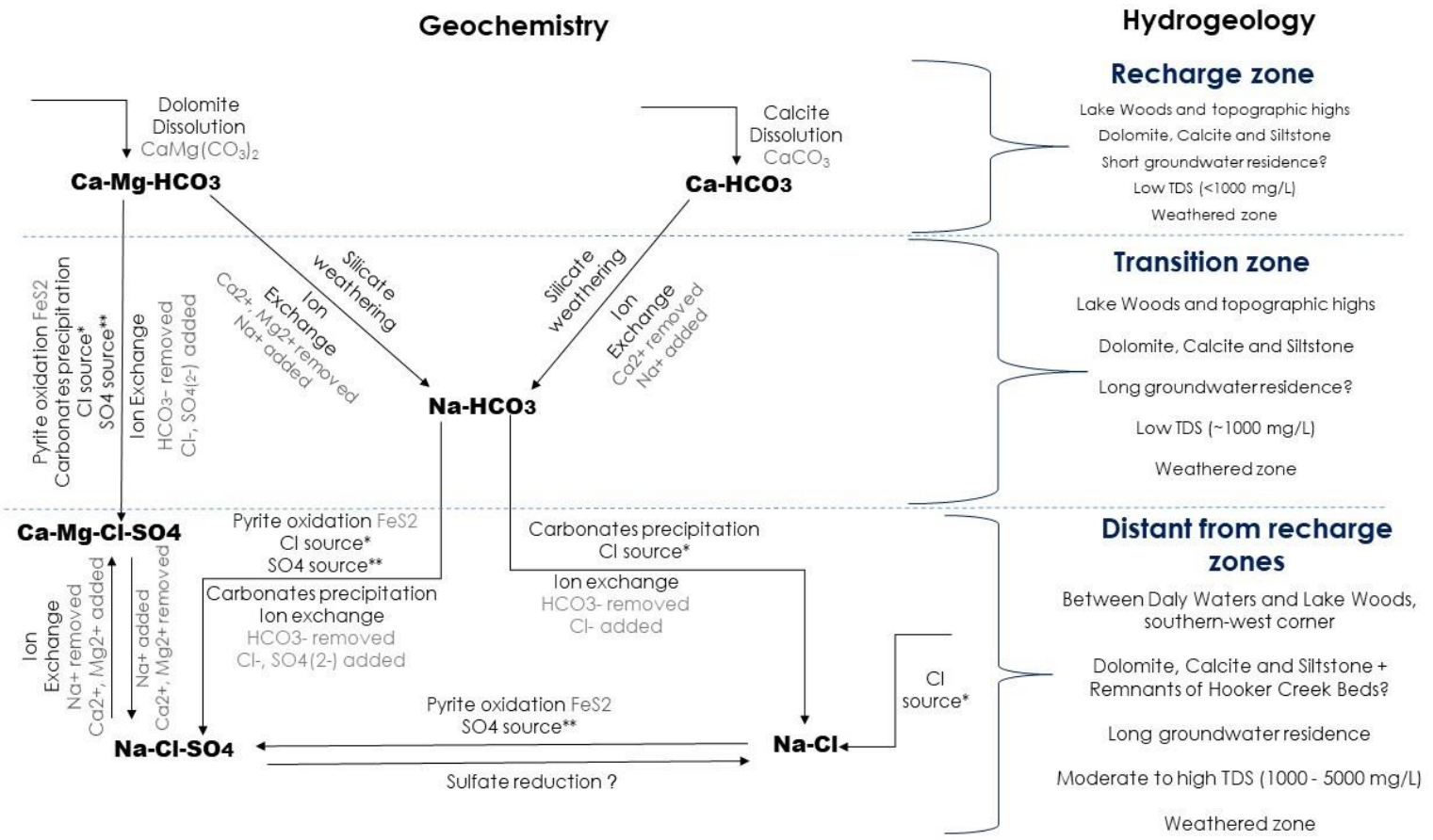

Figure 16 Conceptual model of dominant water-mineral interaction processes along flow paths A-A' and B-B' (Montejinni Limestone aquifer)

Carbonates dissolution and precipitation is occurring at all locations, however this is only indicated in the figure where this process is likely to be significant. Cl source* indicate potential Cl^- cross-formational sources that could be the Hooker Creek Beds Formation, Anthony Lagoon Formation and Basement units. SO_4^{**} source indicate potential cross-formational sources that could be the Hooker Creek Beds Formation and the Anthony Lagoon Formation

5.2 Limitations, uncertainties, and future directions

While this study provides valuable insights into major hydrochemical processes contributing to chemical variations along regional flow paths, caution should be taken when interpreting these results. The methods used in this study elucidate the major hydrogeochemical processes but come with inherent limitations. To gain improved insights in fully understanding the system, the thermodynamics and kinetics processes that can influence the rate, extent and feasibility of these processes need consideration. Further, there are uncertainties related to the impact of water level fluctuations on the hydrochemical data, specifically, the impact of seasonality and large temporal variations in sampling events on the overall water quality. Given the importance of this area and the identified data gaps, it is imperative to implement a regional monitoring program that concurrently collects water levels and water quality data, allowing for an investigation into their temporal and spatial interactions.

Another substantial gap in the present study is the absence of redox potential data in the water quality dataset. Redox potential is a critical parameter for determining the influence of electron donor-acceptor ions that influence the overall water quality such as sulfate/sulphide species through microbial degradation (Appelo and Postma, 1996). To address this gap, it is recommended to include in-situ redox measurements in the monitoring program, which ideally should be measured along with other dynamic parameters such as temperature and pH (e.g., Appello and Postma, 1993). In addition, the laboratory analytical suite should be augmented by the inclusion of dissolved organic carbon and redox active species, such as manganese (Mn), Iron (Fe).

Assuming that hydraulic heads and water quality data used are accurate and relevant, there are many processes that still require confirmation and detailed characterisation. In regions where water composition is attributed to multiple processes, including mixing, recharge conditions and longer residence times (e.g., along A-A' and B-B' flow paths in the Wiso Basin), further investigations such as environmental isotope analyses, mineralogical studies and hydraulic testing, would be instrumental in validating and improving the overall water quality data interpretation.

Additionally, a significant data gap from inadequate monitoring is evident in the central

region of the Wiso Basin to the south of the Buchanan Highway (refer to ***Figure 7***), as previously noted by Shand et al. (2022). Addressing this data gap is crucial, as it would supplement current understanding of flow paths and chemical processes in the southern region, including A-A' and B-B' flow paths and potential spring discharges in the Victoria River catchment to the west.

Despite these limitations and data gaps, this study can serve as an important basis for understanding the evolution of groundwater chemistry and protecting groundwater resources from potential impacts associated with onshore gas development in the Beetaloo region. To improve the understanding of the broader CLA system and the environmental impact assessment process for future onshore gas projects, this study's methodology can be replicated in other regions within the wider CLA. While this study used a single data point for selected bores (~close to average values) to avoid issues with ion balance errors, an alternative approach to use statistically valid dataset is recommended to accommodate short term fluctuations in a broader dataset.

6. CONCLUSION

In conclusion, this study represents an advancement in the current understanding of hydrogeochemical processes within the CLA, particularly in its western region. The key findings of the study provide valuable insights into the complex interactions between groundwater and geological formations, by shedding light on hydrochemical variations and major factors at play. Given the growing interest of the onshore gas industry in the Beetaloo sub-basin, which is part of the study area, this study serves as an important basis for hydrochemical investigation based on major ion composition that may be used as a tool for the future management of this valuable resource.

The modern groundwater potentiometric surface and inferred flow paths presented here reaffirm earlier observations of groundwater flowing from south to north. Additionally, the geochemical similarity observed between Tindall Limestone groundwater and the water discharging into the Flora River indicates that the Flora River springs primarily draw water from the Tindall Limestone aquifer, with a minor contribution from the Jinduckin Formation. Terrain and groundwater elevation analyses also suggest the possibility of westward flow from the Lake Woods area towards the Victoria River Catchment, a phenomenon that warrants further detailed investigation.

The analysis of regional water quality data has identified several processes influencing groundwater composition. These processes include climatic conditions, recharge locations, groundwater residence times, mixing processses and various water-mineral interactions that collectively control the groundwater composition. A comparative assessment of groundwater data with average seawater and rainwater data reveals the dominant role played by interactions between water and rock minerals in influencing the water chemistry, with only marginal effects from ET.

The wide variations in the dominance of major ions along regional flow paths indicate the influence from various hydrogeochemical processes, aligning with the geology of the study area. Geochemical modelling using PHREEQC indicated that the water chemistry is predominantly dolomite and calcite solubility controlled, as supported by the near saturation of these minerals across the CLA. Scatter plots further confirm a minor contribution from silicate hydrolysis and cation

exchange processes to overall water chemistry.

While this study has employed major ion composition as a proxy for understanding geochemical processes, challenges remain in fully identifying the complex interactions and chemical processes at play, particularly along the eastern and southern margins where distinctive high salinity water types (Na-HCO_3, Ca-Mg-Cl-SO_4, Na-Cl-SO_4, and Na-Cl) predominate. This study attributes the plausible origin of distinctive water composition within the areas identified to be associated with a number of processes, including carbonate dissolution and precipitation, cation exchange processes, silicate weathering and pyrite oxidation. Other factors such as cross-formational flow may also be occurring. To address this uncertainty, comprehensive investigations are warranted, which may include environmental isotope analyses, mineralogical studies, and aquifer testing. Future work should also consider simultaneous assessments of water levels and water quality, as this is vital for unravelling the complexity of chemical processes.

REFERENCES

Al Kuisi, M, Abed, AM, Mashal, K, Saffarini, G & Saqhour, F 2015, 'Hydrogeochemistry of groundwater from karstic limestone aquifer highlighting arsenic contamination: case study from Jordan', *Arabian Journal of Geosciences*, vol. 8, no. 11, pp. 9699-9720.

Amery, T & Tickell, S 2022, *Beetaloo Sub-basin SREBA Water Studies: Water level monitoring review for overlying primary aquifers*, Technical Report 20/2022, Department of Environment, Parks and Water Security, Northern Territory Government.

Appelo, CAJ & Postma, D 1996, *Geochemistry, groundwater and pollution*, 2nd edition, Balkema Publishers, The Netherlands.

Australian Bureau of Statistics, n.d., *Search Census Data*, Commonwealth of Australia, viewed 25 July 2023, <https://www.abs.gov.au/census/find-census-data/search-by-area>.

Department of Agriculture, Water and the Environment, 2021, *Geological and Baseline Bioregional Assessment Program: Beetaloo GBA Region*, Australian Government, viewed 10 August 2023, <https://www.bioregionalassessments.gov.au/assessments/geological-and-bioregional-assessment-program/beetaloo-gba-region>.

Barzegar, R, Asghari Moghaddam, A, Nazemi, AH & Adamowski, J 2018, 'Evidence for the occurrence of hydrogeochemical processes in the groundwater of Khoy plain, northwestern Iran, using ionic ratios and geochemical modeling', *Environmental Earth Sciences*, vol. 77, pp.1-17.

BOM (Bureau of Meteorology), 2019, *Groundwater Dependent Ecosystems Atlas*, Australian Government, viewed 2 September 2023, <http://www.bom.gov.au/water/groundwater/gde/map.shtml>.

BOM, 2020, *Maps of average conditions*. Australian Government, viewed 7 July 2023, <http://www.bom.gov.au/climate/averages/maps.shtml>.

Bruwer, Q & Tickell, SJ 2015, *Daly Basin Groundwater Resource Assessment - North Mataranka to Daly Waters*, Report 20/2015, Department of Land Resource Management, Northern Territory Government.

Carroll, S, Hao, Y & Aines, R 2009, 'Geochemical detection of carbon dioxide in dilute aquifers', *Geochemical transactions*, vol. 10, no. 1, pp.1-18.

Clark, ID & Fritz, P 1997, *Environmental Isotopes in Hydrogeology*, 1st edition, CRC Press, New York.

Crosbie, RS & Rachakonda, PK 2021, 'Constraining probabilistic chloride mass-balance recharge estimates using baseflow and remotely sensed ET: the Cambrian Limestone Aquifer in northern Australia', *Hydrogeology Journal*, vol. 29, pp. 1399-1419.

CSIRO (Commonwealth Science and Industrial Research Organisation), 2023, *GISERA*, Australian Government, viewed 10 July 2022, <https://gisera.csiro.au/state/nt/>.

de Caritat, P, Bastrakov, EN, Jaireth, S, English, PM & Clarke, JDA, Mernagh, TP, Wygralak, AS, Dulfer, HE & Trafford, J 2019, 'Groundwater geochemistry, hydrogeology and potash mineral potential of the Lake Woods region, Northern Territory, Australia', *Australian Journal of Earth Sciences*, vol. 66, no., 3, pp. 411-430.

De Vries, JJ & Simmers, I 2002, 'Groundwater recharge: an overview of processes and challenges', *Hydrogeology Journal*, vol. 10, pp. 5-17.

Deloitte, 2020, *Report on the Development of the Beetaloo Subbasin*, report to the Commonwealth Department of Industry, Science, Energy and Resources.

Demlie, M, Wohnlich, S & Ayenew, T 2008,'Major ion hydrochemistry and environmental isotope signatures as a tool in assessing groundwater occurrence and its dynamics in a fractured volcanic aquifer system located within a heavily urbanized catchment, central Ethiopia', *Journal of hydrology*, vol. 353, pp.175-188.

DEPWS (Department of Environment, Parks and Water Security), 2021a, *Northern Territory Groundwater - Aquifer Types,* Northern Territory Government, viewed 20 June 2022, <https://data.nt.gov.au/dataset/northern-territory-ground-water-aquifers>.

DEPWS, 2021b, *SREBA: Scope of works. Water quality and quantity studies for the Beetaloo Sub-basin*. Department of Environment, Parks and Water Security, Northern Territory Government, unpublished.

DEPWS, 2021c, *Bore Sites in the Northern Territory*, Northern Territory Government, viewed 10 December 2022, < https://data.nt.gov.au/dataset/nt-bore-locations-water-quality-and-groundwater-levels >.

DEPWS, 2021d, *Natural Resources Map*, Northern Territory Government, viewed 2 February 2022, <https://nrmaps.nt.gov.au/nrmaps.html>.

DEPWS, 2022a, *Water resources of the Flora water management area*, Technical Report 2/2022, Department of Environment, Parks and Water Security, Northern Territory Government.

DEPWS, 2022b, *Water resources of the Wiso Basin water management area*, Technical Report 6/2022, Department of Environment, Parks and Water Security, Northern Territory Government.

DEPWS, 2022c, *Regional Report: Strategic Regional Environmental and Baseline Assessment for the Beetaloo Sub-basin*, Technical Report 41/2022, Department of Environment, Parks and Water Security, Northern Territory Government.

DEPWS, 2022d, *Water Quality and Quantity Baseline Summary Report: Strategic Regional Environmental and Baseline Assessment for the Beetaloo Sub-basin,* Technical Report 24/2022, Department of Environment, Parks and Water Security, Northern Territory Government.

DEPWS, 2022d, *SREBA Beetaloo groundwater quality database*, Northern Territory Government, viewed 26 August 2023, <https://srebadata.nt.gov.au/view/ntg-sda-000000051>.

DEPWS, 2023a, *SREBA Beetaloo Aquifers*, Northern Territory Government, viewed 26 August 2023, <https://srebadata.nt.gov.au/view/ntg-spa-000000158>.

DEPWS, 2023b, *The NT Water Data WebPortal*, Northern Territory Government, viewed 26 August 2023, <https://ntg.aquaticinformatics.net/Data/Map/Parameter/Measured%20Water%20Level/Statistic/LATESTWATERLEVEL/Interval/Latest>.

DEPWS, 2023c, *Strategic Regional Environmental and Baseline Assessment (SREBA),* Northern Territory Government, viewed 15 July 2023, <https://depws.nt.gov.au/onshore-gas/sreba>.

Deslandes, A, Christoph, G, Lamontagne, S, Wilske, C, Suckow, A 2019, *Environmental Tracers in the Beetaloo Basin*: *Aquifer and groundwater characterization*, CSIRO, Australian Government.

Edmunds, WM & Smedley, PL 2000, 'Residence time indicators in groundwater: the East Midlands Triassic sandstone aquifer', *Applied Geochemistry*, vol. 15, no. 6, pp.737-752.

Engle, MA & Rowan, EL 2013, 'Interpretation of Na–Cl–Br systematics in sedimentary basin brines: comparison of concentration, element ratio, and isometric log-ratio approaches', *Mathematical Geosciences*, vol. 45, no. 1, pp.87-101.

Evans, TJ, Radke, BM, Martinez, J, Buchanan, S, Cook, SB, Raiber, M, Ransley, TR, Lai, ÉCS, Skeers, N, Woods, M, Evenden, C, Cassel, R & Dunn, B 2020, *Hydrogeology of the Beetaloo GBA region*: *Technical appendix for the Geological and Bioregional Assessment: Stage 2. Department of the Environment and Energy*, Bureau of Meteorology, CSIRO and Geoscience Australia, Australian Government.

Foo, DY & Matthews, I 2001, *Hydrogeology of the Sturt Plateau: 1:250 000 Scale Map Explanatory Notes*, Report 17/2000D, Department of Infrastructure, Planning and Environment, Northern Territory Government.

Fulton, S & Knapton, A 2015, *Beetaloo Basin Hydrogeological Assessment*, CloudGMS.

Gabrovšek, F & Dreybrodt, W 2010, 'Karstification in unconfined limestone aquifers by mixing of phreatic water with surface water from a local input: A model', *Journal of hydrology*, vol. 386, no. 1, pp. 130-141.

Gallant, J, Tickle, PK, Wilson, N, Dowling, T & Read, A 2010, *1 second SRTM Level 2 Derived Smoothed Digital Elevation Model (DEM-S) version 1.0.*, Geoscience Australian, viewed 10 August 2023, <https://pid.geoscience.gov.au/dataset/ga/70715>.

Galloway, JN, Likens, GE, Keene, WC & Miller, JM 1982, 'The composition of precipitation in remote areas of the world', *Journal of Geophysical Research: Oceans*, vol. 87, no. C11, pp. 8771-8786.

Gibson, JJ, Edwards, TWD, Birks, SJ, St Amour, NA, Buhay, WM, McEachern, P, Wolfe, BB & Peters, DL 2005, 'Progress in isotope tracer hydrology in Canada', *Hydrological Processes: An International Journal*, vol. 19, no. 1, pp. 303-327.

Gonfiantini, R, Fröhlich, K, Araguás-Araguás, L & Rozanski, K 1998, 'Isotopes in groundwater hydrology', In *Isotope tracers in catchment hydrology*, pp. 203-246.

Gosselin, DC 1997, 'Major-ion chemistry of compositionally diverse lakes, Western Nebraska, U.S.A.: Implications for paleoclimatic interpretations', *Journal of paleolimnology*, vol. 17, no. 1, pp. 33-49.

Han, Y, Wang, G, Cravotta III, CA, Hu, W, Bian, Y, Zhang, Z & Liu, Y 2013,'Hydrogeochemical evolution of Ordovician limestone groundwater in Yanzhou, North China', *Hydrological Processes*, vol. 27, no.

16, pp. 2247-2257.

Hounslow, AW 1995, *Water Quality Data: Analysis and Interpretation*, 1st edition, CRC Press, Lewis Publishers, New York.

Huddlestone-Holmes, CR, Holland, K & Peeters, LJ 2021, 'Geological and Bioregional Assessments: a tale of two basins', *The APPEA Journal*, vol. 61, no. 2, pp. 491-494.

Irvine, D & Duvert, C 2022, *Beetaloo Sub-basin SREBA Water Studies: Flora River groundwater and surface water interactions study*, Technical Report 26/2022, Report to the Northern Territory Department of Environment, Parks and Water Security, Research Institute for the Environment and Livelihoods, Charles Darwin University and the National Centre for Groundwater Research and Training.

Jalali, M 2009, 'Geochemistry characterization of groundwater in an agricultural area of Razan, Hamadan, Iran', *Environmental Geology*, vol. 56, pp.1479-1488.

Jankowski, J & Acworth, RI 1997, 'Impact of debris-flow deposits on hydrogeochemical processes and the developement of dryland salinity in the Yass River Catchment, New South Wales, Australia', *Hydrogeology Journal*, vol. 5, pp. 71-88.

Karp, D 2002, *Land degradation associated with sinkhole development in the Katherine Region*, Technical Report 11/2002, Department of Infrastructures, Planning and Environment, Northern Territory Government.

Kennewell, PJ & Huleatt, MB 1980, *Geology of the Wiso Basin, Northern Territory*, Bulletin 205, Bureau of Mineral Resources, Geology and Geophysics, Department of Natural Development and Energy, Australian Government Publishing Service, Canberra.

Keywood, M 1995, 'Origins and sources of atmospheric precipitation from Australia: Chlorine-36 and major-element chemistry', PhD thesis, Australian National University, Canberra, Australia.

Knapton, A 2020, *Upgrade of the Coupled Model of the Cambrian Limestone Aquifer and Roper River Systems*, Report to the Department of Environment and Natural Resources, CloudGMS.

Kowalska, M, Güler, H & Cocke, DL 1994, 'Interactions of clay minerals with organic pollutants', *Science of the total environment*, vol. 141, pp. 223-240.

Kruse, PD & Munson, TJ 2013, 'Chapter: Daly Basin' in Ahmad, M & Munson, TJ (ed), *Geology and mineral resources of the Northern Territory*, Northern Territory Geological Survey, Northern Territory Government.

Leather, DT, Bahadori, A, Nwaoha, C & Wood, DA 2013, 'A review of Australia's natural gas resources and their exploitation', *Journal of Natural Gas Science and Engineering*, vol. 10, pp. 68-88.

Lewis, S, Evans, T, Pavey, C, Holland, K, Henderson, B, Kilgour, P, Dehelean, A, Karim, F, Viney, N, Post, D, Schmidt, R, Sudholz, C, Brandon, C, Zhang, Y, Lymburner, L, Dunn, B, Mount, R, Gonzalez, D, Peeters, L, O'Grady, A, Dunne, R, Ickowicz, A, Hosack, G, Hayes, K, Dambacher, J & Barry, S 2018, *Impact and risk analysis for the Galilee subregion*, Department of the Environment and Energy, Bureau of Meteorology, CSIRO and Geoscience Australia, Australian Government.

Love, AJ 2003, 'Groundwater flow and solute transport dynamics in a fractured meta-sedimentary aquifer', PhD thesis, Flinders University, Adelaide, Australia.

Maloney. KO, Baruch-Mordo, S, Patterson LA, Nicot, JP, Entrekin, SA, Fargione, JE, Kiesecker, JM, Konschnik, KE, Ryan, JN, Trainor, AM & Saiers, JE 2017, 'Unconventional oil and gas spills: Materials, volumes, and risks to surface waters in four states of the US', *Science of the Total Environment*, vol. 581, pp. 369-377.

Mayo, AL & Loucks, MD 1995, 'Solute and isotopic geochemistry and ground water flow in the central Wasatch Range, Utah', *Journal of Hydrology*, vol. 172, pp. 31-59.

Mustapha, A & Aris, AZ 2012, 'Spatial aspects of surface water quality in the Jakara Basin, Nigeria using chemometric analysis', *Journal of environmental science and health*, vol. 47, no. 10, pp. 1455-1465.

Northern Territory Government, n.d., *Open Data Portal*, Northern Territory Government, viewed 4 July 2023, < https://data.nt.gov.au/>.

Origin Energy Resources Limited, 2016, *Hydraulic stimulation and well testing EP: Amungee NW-1H, and Beetaloo W-1 OR Nutwood Downs SW-1*, Report CDN/ID NT-2050-35-PH-0018, Origin.

Orr, ML, Bernardel, G, Owens, R, Hall, LS, Skeers, N, Reese, B & Woods, M 2020, *Geology of the Beetaloo GBA region. Technical appendix for the Geological and Bioregional Assessment: Stage 2*, Department of the Environment and Energy, Bureau of Meteorology, CSIRO and Geoscience Australia, Australian Government.

Papoulias, DM & Velasco, AL 2013, 'Histopathological analysis of fish from Acorn Fork Creek, Kentucky,

exposed to hydraulic fracturing fluid releases', *Southeastern Naturalist*, vol. 12, pp. 92–111.

Parkhust, DL & Appelo, CAJ 1999, *A computer program for speciation, batch-reaction, one-dimensional transport and inverse geochemical calculations*, Water Resources Investigation, US Geological Survey, the United States Government.

Patterson, LA, Konschnik, KE, Wiseman, H, Fargione, J, Maloney, KO, Kiesecker, J, Nicot, JP, Baruch-Mordo, S, Entrekin, S, Trainor, A & Saiers, JE 2017, 'Unconventional oil and gas spills: risks, mitigation priorities, and state reporting requirements', *Environmental science & technology*, vol. 51, *no.* 5, pp. 2563-2573.

Pepper, R, Anderson, A, Ashworth, P, Beck, V, Hart, B, Jones, D, Priestly, B, Ritchie, D & Smith, R 2018, *Final report of the scientific inquiry into hydraulic fracturing in the Northern Territory*, Report to the Chief Minister of the Northern Territory, The scientific inquiry into hydraulic fracturing in the Northern Territory.

Piper, AM 1944, 'A graphic procedure in the geochemical interpretation of water-analyses', *Eos, Transactions American Geophysical Union*, vol. 25, no. 6, pp. 914-928.

Randal, MA 1967, *Groundwater in the Barkly Tableland, Northern Territory*, Bulletin 91, Bureau of Mineral Resources, Geology and Physics, Australian Government Publishing Service, Canberra.

Randal, MA 1973, *Groundwater in the Northern Wiso Basin and Environs, Northern Territory*, Bulletin 123, Department of Minerals & Energy, Bureau of Mineral Resources, Geology & Geophysics, Australian Government Publishing Service, Canberra.

Schroder, I, de Caritat, P, Wallace, L, Trihey, J, Tobin, J, Boreham, C, English, P, Sohn, J, Palatty, P, Coghlan, R, Flower, C, Maher, P, Thorose, MD, Long, I, Byass, J & Jinadasa, N 2020, *Northern Australia Hydrogeochemical Survey: final data release and hydrogeochemical atlas for Exploring for the Future*, Record 2020/15, Geoscience Australia, Australian Government.

Scrimgeour, I 2016, *Summary of current knowledge of petroleum geology, shale gas resources and exploration in the Beetaloo Sub-basin*, report to the Scientific Inquiry into Hydraulic Fracturing in the Northern Territory, Northern Territory Geological Survey, Northern Territory Government.

Shamsalsadati, S, Allen, T, Comoglu, M & Glanville, H 2022, *The Beetaloo Sub-basin Baseline Seismic Monitoring Project – Phase 1 Observations*, Geoscience Australia, Australian Government.

Shand, P, Love, AJ & Maggu, J 2022, *Beetaloo Sub-basin SREBA Water Studies: Review of regional groundwater quality*, Technical Report 35/2022, Department of Environment, Parks and Water Security, Northern Territory Government.

Sheikhy Narany, T, Ramli, MF, Aris, AZ, Sulaiman, WNA, Juahir, H & Fakharian, K 2014, 'Identification of the hydrogeochemical processes in groundwater using classic integrated geochemical methods and geostatistical techniques, in Amol-Babol Plain, Iran', *The Scientific World Journal*, vol. 2014, pp. 15.

Siegel, D 2008, 'Reductionist hydrogeology: ten fundamental principles', *Hydrological Processes: An International Journal*, vol. 22, no. 25, pp. 4967-4970.

Smith, BR 2016, *HyLogger drillhole report for NDW12-01 'Daly Waters', McArthur Basin, Northern Territory*, HyLogger Data Package 0058, Northern Territory Geological Survey, Northern Territory Government.

Southby, C, Rollet, N, Carson, C, Carr, L, Henson, P, Fomin, T, Costelloe, R, Doublier, M & Close, D 2021, *The Exploring for the Future 2019 Barkly Reflection Seismic Survey: Key discoveries and implication for resources*, Geoscience Australia, Australian Government.

Southby, C, Carson, CJ, Fomin, T, Rollet, N, Henson, PA, Carr, LK, Doublier, MP & Close, D 2022, *Exploring for the Future - The 2019 Barkly Reflection Seismic Survey (L212),* Geoscience Australia, Australian Government.

Staben G & Edmeades, B 2017, *Northern Territory Land Use Mapping for Biosecurity 2016*, Technical Report 18/2017D, Department of Environment and Natural Resources, Northern Territory Government.

Suckow, A, Deslandes, A, Gerber, C & Lamontagne, S 2018, *Environmental tracers in the Beetaloo Sub-basin*, CSIRO, Australian Government.

TERC (Territory Economic Reconstruction Commission), 2020, *A Step Change to win investment and create jobs: Territory Economic Reconstruction Commission: Final Report*, NT Rebound, Northern Territory Government.

Tickell, SJ 2005, *Groundwater Resources of the Tindall Limestone*, Department of Natural Resources the Environment and the Arts, Northern Territory Government.

Tickell, SJ 2008, *Explanatory notes to the Groundwater Map of the Northern Territory*, Technical Report No.

12/2008D, Department of Natural Resources the Environment The Arts and Sport, Northern Territory Government.

Tickell, SJ 2009, *Groundwater in the Daly Basin*, Technical Report No. 27/2008D, Department of Natural Resources the Environment The Arts and Sport, Northern Territory Government.

Tickell, SJ (editor) 2011, *Assessment of major spring systems in the Oolloo Dolostone, Daly River*, Technical Report No. 22/2011D, Department of Natural Resources, Environment The Arts and Sport, Northern Territory Government.

Tickell, SJ & Bruwer, Q 2017, *Georgina Basin Groundwater Assessment: Daly Waters to Tennant Creek*, Technical Report 17/2017, Department of Environment and Natural Resources, Northern Territory Government.

Tickell, SJ 2018, *Hydrogeology of the Jinduckin Formation, Florina Rd, Katherine*, Technical Report 28/2018, Department of Environment and Natural Resources, Northern Territory Government.

Tickell, SJ 2022, *Beetaloo Sub-basin SREBA Water Studies: Aquifer mapping and summary report*, Technical Report 19/2022, Department of Environment, Parks and Water Security, Northern Territory Government.

Verma, MN & Jolly, PB 1992, *Hydrogeology of Helen Springs: Explanatory Notes for 1:250 000 Scale Map*, Report 50/1992, Power and Water Authority, Northern Territory Government.

Wallace, L, Schroder, I, de Caritat, P. English, P, Boreham, C, Sohn, J, Palatty, P & Czarnota, K 2018, *Northern Australia Hydrogeochemical Survey: Data release, Preliminary Interpretation and Atlas – Tennant Creek, McArthur River and Lake Woods regions*, Record 2018/48, Geoscience Australia, Canberra.

Wilkes, P, Rachakonda, PK, Larcher, A & Woltering, M 2019, *Baseline assessment of groundwater characteristics in the Beetaloo Sub-basin, NT*, Geochemistry Analysis report to the Gas Industry Social and Environmental Research Alliance (GISERA), CSIRO, Australia.

Wilkins, A, Crosbie, R, Louth-Robins, T, Davies, P, Raiber, M, Dawes, W & Gao, L, 2022, 'Australian gridded chloride deposition-rate dataset', *Data in Brief*, vol. 42, pp.108-189.

APPENDICES

Appendix 1: Data quality assessment and filtration

Matrix used for data quality assessment: Matrix used as below classified each sample into five categories: excellent, good, fair, poor and unsuitable

Parameters / Data quality	Sampling Method	Ion balance error	Known screen depth/Aquifer	Intercepted Aquifers
Excellent	Pumping	<5%	Yes	Single
Good	Pumping	5-10%	Yes	Single
Fair	Pumping	10-15%	Yes	Single
Poor	Pumping/Airlifting	1-15%	Yes/No	Unknown/Single/Multiple
Unsuitable	Pumping/Airlifting	>15%	Yes/No	Single/Multiple

Water quality data ranking for sampled data:

Quality assurance analysis found 77 bores not achieving the excellent water quality ranking at any time. Of these, 4 are screened in the Jinduckin Formation aquifer, 23 in the Tindall Limestone aquifer, 32 in the Montejinni Limestone aquifer, 11 in multiple aquifers and 7 bores in unknown (no information available) aquifers.

		Data Ranking				
	Total Count	***Excellent***	***Good***	***Fair***	***Poor***	***Unsuitable***
Bores sampled	*214*	137	8	2	59	8
Sample Counts	*711*	285	31	10	104	281
Targeted Aquifers						
Jinduckin Formation	*32*	17	1	1	11	2
Tindall Limestone	*116*	50	11	2	44	9
Montejinni Limestone	*563*	218	19	7	49	270

Appendix 2: Bores selected for analysis

ID	Bore	Sample date	Latitude	Longitude	Aquifer	Basin
1	RN027072	18/07/1990	-14.92	131.89	Jinduckin Formation	Daly
2	RN007245	2/10/1970	-14.93	132.25	Jinduckin Formation	Daly
3	RN008242	22/08/1984	-14.86	131.84	Jinduckin Formation	Daly
4	RN007881	30/10/1985	-14.83	131.72	Jinduckin Formation	Daly
5	RN007095	14/06/1985	-14.86	131.84	Jinduckin Formation	Daly
6	RN028162	15/04/1993	-14.81	131.61	Jinduckin Formation	Daly
7	RN007882	5/02/1988	-14.95	131.84	Jinduckin Formation	Daly
8	RN006767	30/09/1999	-14.91	132.35	Jinduckin Formation	Daly
9	RN005007	30/10/1985	-14.92	131.88	Jinduckin Formation	Daly
10	RN041543	2/10/2021	-15.19	132.78	Tindall Limestone	Daly
11	RN028626	15/09/1998	-14.81	131.50	Tindall Limestone	Daly
12	RN027795	16/09/1998	-14.93	131.61	Tindall Limestone	Daly
13	RN032166	5/10/2021	-15.53	132.65	Tindall Limestone	Daly
14	RN029769	28/05/1999	-15.63	132.68	Tindall Limestone	Daly
15	RN031926	25/08/2015	-15.86	132.68	Tindall Limestone	Daly
16	RN000903	1/07/1969	-15.23	132.26	Tindall Limestone	Daly
17	RN031390	6/08/1998	-15.07	131.79	Tindall Limestone	Daly
18	RN023859	2/10/2021	-15.41	132.68	Tindall Limestone	Daly
19	RN024784	1/10/2021	-15.88	132.41	Tindall Limestone	Daly
20	RN000906	1/07/1969	-15.86	132.05	Tindall Limestone	Daly
21	RN006745	3/06/1998	-15.72	132.59	Tindall Limestone	Daly
22	RN026113	2/10/2021	-15.19	132.78	Tindall Limestone	Daly
23	RN032169	25/10/1999	-15.61	132.61	Tindall Limestone	Daly
24	RN031382	18/10/2018	-15.37	132.65	Tindall Limestone	Daly
25	RN006845	5/06/1998	-15.42	132.27	Tindall Limestone	Daly
26	RN026116	3/06/1998	-15.41	132.23	Tindall Limestone	Daly
27	RN031617	9/06/1998	-15.57	132.48	Tindall Limestone	Daly
28	RN027337	28/05/1999	-15.78	132.58	Tindall Limestone	Daly
29	RN030656	21/08/1996	-15.83	132.59	Tindall Limestone	Daly
30	RN027611	12/06/1991	-14.81	131.54	Tindall Limestone	Daly
31	RN005928	9/07/1992	-15.69	132.73	Tindall Limestone	Daly
32	RN027610	16/09/1998	-14.81	131.54	Tindall Limestone	Daly
33	RN031108	15/06/1998	-15.17	132.18	Tindall Limestone	Daly
34	RN035131	12/10/2021	-15.53	132.87	Tindall Limestone	Daly
35	RN031391	15/08/1998	-15.12	132.10	Tindall Limestone	Daly
36	RN031387	11/08/1998	-14.76	131.60	Tindall Limestone	Daly
37	RN022101	20/06/1986	-15.25	132.15	Tindall Limestone	Daly
38	RN024612	19/06/1986	-15.24	132.12	Tindall Limestone	Daly
39	RN030710	12/09/1997	-16.05	132.92	Tindall Limestone	Daly
40	RN028180	1/06/1992	-15.84	132.05	Tindall Limestone	Daly
41	RN031381	12/06/1998	-15.18	132.50	Tindall Limestone	Daly
42	RN031480	18/11/1997	-15.03	132.63	Tindall Limestone	Daly
43	RN032162	9/09/1999	-15.57	132.41	Tindall Limestone	Daly
44	RN027124	11/11/1990	-15.21	132.42	Tindall Limestone	Daly
45	RN027794	24/11/1997	-15.27	132.91	Tindall Limestone	Daly
46	RN030695	13/03/1997	-15.30	132.26	Tindall Limestone	Daly
47	RN007246	30/09/1999	-14.93	132.30	Tindall Limestone	Daly
48	RN031618	8/06/1998	-15.57	132.37	Tindall Limestone	Daly
49	RN035146	19/10/2018	-15.68	132.75	Tindall Limestone	Daly

ID	Bore	Sample date	Latitude	Longitude	Aquifer	Basin
50	RN027341	10/10/2021	-16.54	132.99	Montejinni Limestone	Wiso
51	RN041443	15/09/2020	-16.32	132.74	Montejinni Limestone	Wiso
52	RN030870	5/06/1998	-16.49	133.06	Montejinni Limestone	Wiso
53	RN001982	6/06/1998	-16.40	132.80	Montejinni Limestone	Wiso
54	RN030871	24/08/1999	-16.38	132.99	Montejinni Limestone	Wiso
55	RN000589	6/10/1994	-16.84	132.81	Montejinni Limestone	Wiso
56	RN025209	13/01/1995	-16.20	133.09	Montejinni Limestone	Wiso
57	RN031606	26/08/1999	-16.03	133.04	Montejinni Limestone	Wiso
58	RN032464	11/09/2000	-16.29	132.88	Montejinni Limestone	Wiso
59	RN004518	30/06/1969	-16.42	132.09	Montejinni Limestone	Wiso
60	RN020020	20/11/1979	-16.64	131.93	Montejinni Limestone	Wiso
61	RN030655	15/08/1996	-16.16	132.89	Montejinni Limestone	Wiso
62	RN000512	20/10/1995	-16.75	131.65	Montejinni Limestone	Wiso
63	RN024816	14/05/1987	-16.74	132.39	Montejinni Limestone	Wiso
64	RN020019	8/11/1979	-16.64	131.93	Montejinni Limestone	Wiso
65	RN031963	8/09/2000	-16.27	132.60	Montejinni Limestone	Wiso
66	RN026441	10/08/1992	-17.10	131.58	Montejinni Limestone	Wiso
67	RN000588	25/06/1969	-16.77	132.56	Montejinni Limestone	Wiso
68	RN024815	4/05/1987	-16.76	132.77	Montejinni Limestone	Wiso
69	RN000587	25/06/1969	-16.76	132.34	Montejinni Limestone	Wiso
70	RN007432	13/11/1985	-16.71	132.28	Montejinni Limestone	Wiso
71	RN024817	11/05/1987	-16.75	132.57	Montejinni Limestone	Wiso
72	RN031243	27/10/2018	-16.65	133.01	Montejinni Limestone	Wiso
73	RN021783	7/06/1998	-16.17	133.13	Montejinni Limestone	Wiso
74	RN008514	7/06/1998	-16.03	133.14	Montejinni Limestone	Wiso
75	RN005702	30/06/1969	-16.35	132.22	Montejinni Limestone	Wiso
76	RN026205	4/06/1998	-16.35	132.22	Montejinni Limestone	Wiso
77	RN000852	12/08/1992	-17.68	131.41	Montejinni Limestone	Wiso
78	RN006327	10/10/2000	-17.19	133.37	Montejinni Limestone	Wiso
79	RN040363	4/10/2021	-16.72	133.12	Montejinni Limestone	Wiso
80	RN006875	11/01/1970	-16.81	132.23	Montejinni Limestone	Wiso
81	RN000908	25/06/1969	-16.66	132.01	Montejinni Limestone	Wiso
82	RN000586	4/06/1998	-16.74	132.17	Montejinni Limestone	Wiso
83	RN026369	7/08/1992	-17.83	131.30	Montejinni Limestone	Wiso
84	RN001988	28/10/1995	-16.48	131.94	Montejinni Limestone	Wiso
85	RN027331	5/06/1998	-16.55	132.90	Montejinni Limestone	Wiso
86	RN006341	26/05/1994	-17.98	133.59	Montejinni Limestone	Wiso
87	RN002350	27/05/1994	-17.84	133.43	Montejinni Limestone	Wiso
88	RN005690	9/10/2000	-17.70	133.37	Montejinni Limestone	Wiso
89	RN022332	26/05/1994	-18.10	133.50	Montejinni Limestone	Wiso
90	RN034345	9/11/2020	-17.36	133.38	Montejinni Limestone	Wiso
91	RN034344	9/11/2020	-17.36	133.39	Montejinni Limestone	Wiso
92	RN005687	8/09/2013	-17.81	133.30	Montejinni Limestone	Wiso
93	RN025709	9/10/2000	-17.61	133.24	Montejinni Limestone	Wiso
94	RN005686	21/05/1994	-17.92	133.26	Montejinni Limestone	Wiso
95	RN006579	8/09/2013	-17.98	133.36	Montejinni Limestone	Wiso
96	RN026490	8/08/1992	-17.37	131.64	Montejinni Limestone	Wiso
97	RN005689	9/10/2000	-17.64	133.39	Montejinni Limestone	Wiso
98	RN022832	8/06/1994	-17.66	133.49	Montejinni Limestone	Wiso
99	RN001899	20/11/2012	-17.37	133.41	Montejinni Limestone	Wiso
100	RN006336	7/09/2013	-18.08	133.41	Montejinni Limestone	Wiso

ID	Bore	Sample date	Latitude	Longitude	Aquifer	Basin
101	RN022336	21/05/1994	-17.98	133.33	Montejinni Limestone	Wiso
102	RN005688	9/10/2000	-17.54	133.38	Montejinni Limestone	Wiso
103	RN006241	12/05/1984	-17.77	131.40	Montejinni Limestone	Wiso
104	RN022330	21/05/1994	-18.09	133.42	Montejinni Limestone	Wiso
105	RN022232	11/10/2000	-17.36	133.37	Montejinni Limestone	Wiso
106	RN026491	8/08/1992	-17.46	131.64	Montejinni Limestone	Wiso
107	RN000592	17/08/1970	-17.09	133.23	Montejinni Limestone	Wiso
108	RN025708	27/05/1994	-17.54	133.30	Montejinni Limestone	Wiso
109	RN000853	12/05/1984	-17.71	131.49	Montejinni Limestone	Wiso
110	RN022329	8/09/2013	-18.00	133.29	Montejinni Limestone	Wiso
111	RN004579	10/12/1959	-17.28	133.23	Montejinni Limestone	Wiso
112	RN024446	27/05/1994	-17.88	133.22	Montejinni Limestone	Wiso
113	RN009196	8/10/1996	-17.37	133.41	Montejinni Limestone	Wiso
114	RN028416	13/10/2000	-17.37	133.41	Montejinni Limestone	Wiso
115	RN027345	12/11/2013	-17.37	133.41	Montejinni Limestone	Wiso
116	RN021115	8/07/1983	-17.06	133.34	Montejinni Limestone	Wiso
117	RN002263	22/01/1980	-16.91	133.35	Montejinni Limestone	Wiso
118	RN032146	1/05/1999	-17.00	133.38	Montejinni Limestone	Wiso
119	RN027691	7/08/1992	-17.93	131.38	Montejinni Limestone	Wiso
120	RN006648	20/11/1969	-18.53	133.58	Montejinni Limestone	Wiso
121	RN024520	7/08/1992	-17.85	131.53	Montejinni Limestone	Wiso
122	RN036654	27/10/2018	-16.79	132.98	Montejinni Limestone	Wiso
123	RN023713	5/06/1998	-16.72	133.12	Montejinni Limestone	Wiso
124	RN021159	17/10/1995	-16.82	131.85	Montejinni Limestone	Wiso
125	RN026445	17/10/1995	-16.74	131.96	Montejinni Limestone	Wiso
126	RN023174	12/08/1992	-17.69	131.60	Montejinni Limestone	Wiso
127	RN023348	7/08/1992	-17.85	131.41	Montejinni Limestone	Wiso
128	RN006096	25/07/1983	-17.01	133.28	Montejinni Limestone	Wiso
129	RN029380	10/10/2000	-17.31	133.17	Montejinni Limestone	Wiso
130	RN023376	9/06/1994	-17.31	133.17	Montejinni Limestone	Wiso
131	RN024444	26/04/1986	-17.42	133.26	Montejinni Limestone	Wiso
132	RN000590	25/06/1969	-16.95	133.05	Montejinni Limestone	Wiso
133	RN023347	12/08/1992	-17.84	131.62	Montejinni Limestone	Wiso
134	RN006340	1/07/1983	-17.99	133.51	Montejinni Limestone	Wiso
135	RN000218	26/05/1994	-17.74	133.43	Montejinni Limestone	Wiso
136	RN024445	7/07/1994	-17.77	133.20	Montejinni Limestone	Wiso
137	RN023374	11/09/2013	-17.28	133.23	Montejinni Limestone	Wiso

Appendix 3: Normalised ionic ratios plots for SiO2 and HCO3-

(a) SiO_2/Cl^- versus Cl^- (b) HCO_3^-/Cl^- versus Cl^-. SWDL is sea water dilution line (solid line). Samples are plotted on a logarithm scale and units are mmol/L. Samples above the SWDL indicate contributions from water-mineral interaction.

(a)

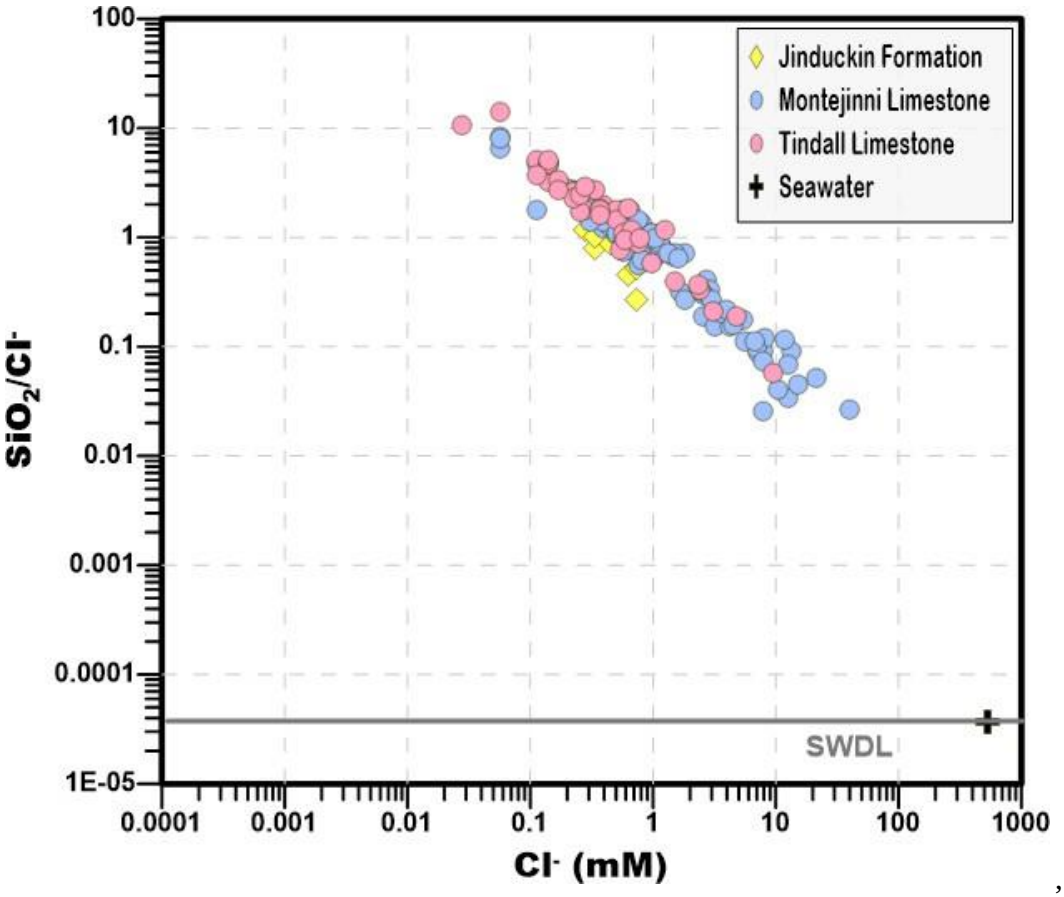

(b)